RSC Advances

REVIEW

View Article Online
View Journal | View Issue

Check for updates

Cite this: *RSC Adv.*, 2024, **14**, 24797

Recent progress in high-voltage P2-Na_xTMO_2 materials and their future perspectives

Manni Li,[a] Weiqi Lin,[a] Yurong Ji,[a] Lianyu Guan,[a] Linyuan Qiu,[a] Yuhong Chen,[a] Qiaoyu Lu[a] and Xiang Ding *[abc]

Received 2nd July 2024
Accepted 19th July 2024

DOI: 10.1039/d4ra04790g

rsc.li/rsc-advances

P2-type layered materials (Na_xTMO_2) have become attractive cathode electrodes owing to their high theoretical energy density and simple preparation. However, they still face severe phase transition and low conductivity. Current research on Na_xTMO_2 is mostly focused on the modification of bulk materials, and the application performances have been infrequently addressed. This review summarizes the information on current common P2-Na_xTMO_2 materials and discusses their sodium-storage mechanisms. Furthermore, modification strategies to improve their performance are addressed for practical applications based on a range of key parameters (output voltage, specific capacity, and lifespan). We also discuss the future development trends and application prospects for P2 cathode materials.

1. Introduction

To date, lithium-ion batteries (LIBs) have been extensively developed and applied in many areas, thus playing a key role in supporting the development of society. However, the low abundance (20 ppm), difficult exploitation and low recovery rates of lithium resources limit LIBs from meeting the requirements of wearable equipment, electric cars (ECs), smart grids and plant-scale energy-storage devices. SIBs have emerged as an alternative and have attracted widespread attention owing to the abundance of Na resources. SIBs are expected to replace LIBs in many fields, and research on them is growing rapidly.

Cathode materials profoundly affect the prime costs and capability of SIBs; therefore, researching and developing low-cost and long-life cathode materials is crucial for the development of SIBs. Such cathode materials include layered transition metal oxides (LTMOs),[1–10] tunnel-type oxides,[11–20] iron–fluorine-based Prussian blue analogues (PBAs)[9,10,21–29] and polyanionic compounds.[10,30–40] Among these, LTMOs have a higher specific capacity and energy density (Table 1).

Layered Na_xTMO_2 (Co, Fe, Mn, Ni, Ti, and Cr) is an embedded or intercalated compound. Delmas *et al.* first proposed the arrangement of Na^+ between TMO_6 layers and divided it into P phase and O phase.[45] As shown in Fig. 1, the number following O or P represents the stacking arrangement of oxygen elements, where Na^+ in P-phase Na_xTMO_2 occupies the triangular prism

Manni Li

Manni Li is an undergraduate student majoring in Applied Chemistry at the College of Chemistry and Materials Science, Fujian Normal University. Her research interests are high-voltage P2-Na_xTMO_2 materials for sodium-ion batteries.

Xiang Ding

Xiang Ding is a professor of the College of Chemistry and Materials Science at Fujian Normal University. He received his bachelor's degree from Jilin University (JLU) in 2015 and PhD from University of Science and Technology of China (USTC) in 2020. His research interests focus on the materials and systems for secondary batteries. He has published more than 30 research papers.

---

[a] College of Chemistry and Materials Science, Fujian Normal University, Fuzhou 350007, China. E-mail: dingx@fjnu.edu.cn

[b] Fujian Provincial Key Laboratory of Advanced Inorganic Oxygenated Materials, College of Chemistry, Fuzhou University, Fuzhou 350108, China

[c] Key Laboratory of Advanced Energy Materials Chemistry (Ministry of Education), Nankai University, Tianjin 300071, China

Table 1 Comparison of some selected cathodes

Materials	Voltage (V)	1st capacity (mA h g^{-1})	Lifespan (%@cycles)	Ref.
$Na_{0.67}Ni_{0.33}Mn_{0.67}O_2$	2.5–4.35	150	90%@100	41
$Na_{0.44}MnO_2$	2.0–3.8	113	82.3%@200	42
$Na_2Mn[Fe(CN)_6]$	2.0–4.2	154	43.2% @100	43
$Na_3V_2(PO_4)_3$	2.3–4.1	85.6	65.5%@100	44

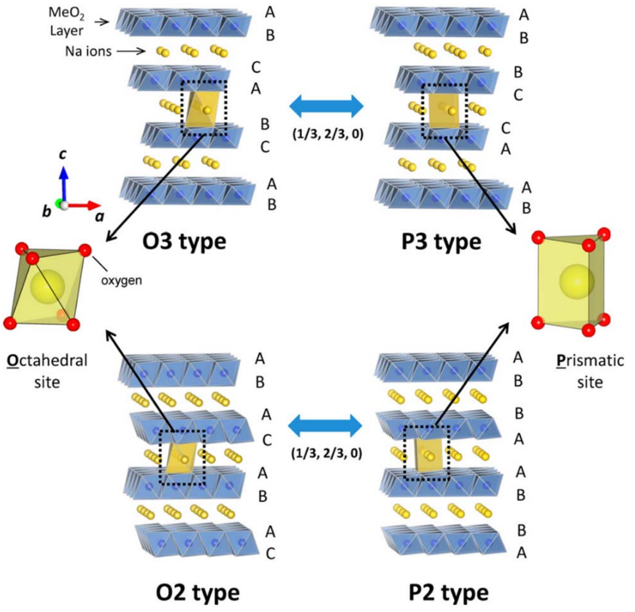

Fig. 1 Classification of Na–TM–O electrodes with TMO_6-octahedra and phase transformation. Adapted with permission from ref. 46, Copyright {2014} American Chemical Society.[46]

gap position, while Na^+ in O-phase Na_xTMO_2 occupies the octahedral gap position between TMO_6 layers.[46] Compared with other materials, P2 layered materials have a higher discharge capacity,[47,48] better cycling stability, and superior ionic conductivity at low Na^+ concentrations.[49,50] Na_xTMO_2 is commonly prepared *via* solid-phase, sol–gel and hydrothermal methods. The most common method is the high-temperature solid-phase method, through which powder particles are prepared without agglomeration *via* a good filling and simple preparation process. However, the powder is not fine enough and is easily mixed with impurities. When constructing the P2 phase, this may cause a slippage of the layer interface. Compared to the solid-phase method, the sol–gel method allows for an easier chemical reaction and requires a lower synthesis temperature. Further, homogeneous mixing between reactant molecules during the formation of a gel leads to the better air stability of Na_xTMO_2. The hydrothermal method is less common as it requires higher humidity, temperature and pressure. However, it yields a product with high purity, which is favorable for the cyclic stability of Na_xTMO_2. In operation, Ni-based P2 phase cathodes have a Ni^{2+}/Ni^{4+} redox couple with high voltage plateaus, such as P2-$Na_{2/3}Ni_{1/3}Mn_{2/3}O_2$ with an average voltage of 3.6 V. Besides, an unfavorable P2–O2 phase transition will occur at a 4.22 V high voltage, which can lead to volume shrinkage and particle cracks appearing during repeated cycling. Electrochemically active (Co^{3+} and Fe^{3+}) and inactive ($Li^+/Zn^{2+}/Mg^{2+}/Al^{3+}/Ti^{4+}$) cationic substitutions have been adopted to tackle these issues. This paper summarizes the information on P2-Na_xTMO_2 and the modification of such materials containing unitary, binary, ternary, and multi-components, with an aim to outline and clarify the current research and look forward to their further development trends and future prospects (Fig. 2).

2 Progress of P2-type materials

2.1 Unitary Na_xTMO_2

Initially, researchers studied single transition metal oxide cathode materials, such as $NaCoO_2$,[51–54] $NaCrO_2$,[54–57] and $NaNiO_2$,[54,58] drawing on such cathode materials that are widely used in LIBs ($LiCoO_2$,[59–61] $LiCrO_2$,[62] and $LiNiO_2$,[63–65] *etc.*). Because of the larger radius of sodium ions ($Na^+ : Li^+ = 108 : 76$ pm), Na^+ diffusion is harder and can result in structure collapse. Therefore, designing a more suitable structure (*e.g.*, larger lattice parameters) for Na^+ (de)intercalation would be desirable.[66]

P2-type Na_xCoO_2 is endowed with a simple structure and competitive capacity.[67] More importantly, compared to

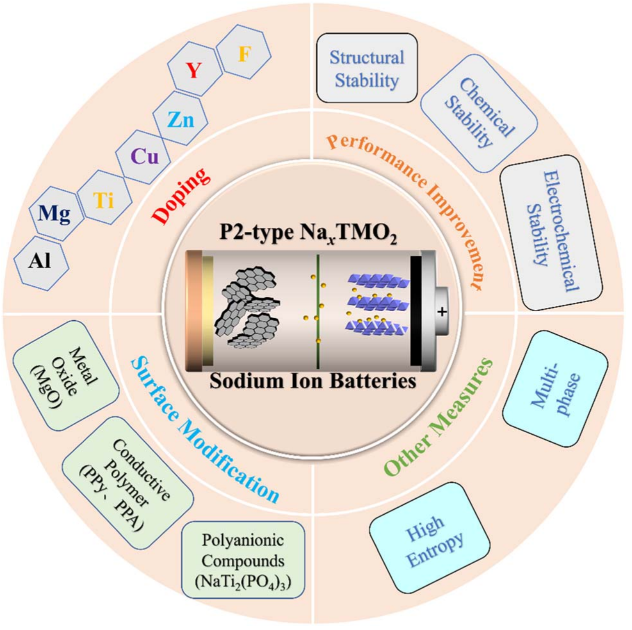

Fig. 2 Schematic of the modification strategies for P2-Na_xTMO_2 cathode materials for SIBs.

commercial $LiCoO_2$, the Na^+ diffusion (D_{Na^+}) for the Na_xCoO_2 electrode ($0.5–1.5 \times 10^{-11}$ cm^{-2} s^{-1}) is better than Li^+ diffusion in the $LiCoO_2$ electrode (1×10^{-11} cm^{-2} s^{-1}).[68] Therefore, increasing D_{Na^+} in this type of material has become a research hotspot. Microspherical P2-Na_xCoO_2 (S-NCO) possesses an inferior specific surface (~2.82 m^2 g^{-1}) area and layered structure,[69] and also exhibits competitive electrochemical stability (82.2 mA h g^{-1} @300 cycles@720 mA g^{-1}). For obtaining single-phase domains in P2-$NaCrO_2$, Gan *et al.* constructed Na^+ vacancy ordering by a deiodination method, demonstrating the system's multiple voltage mechanism.[70] They also proved that structural relaxation as well as electron transfer were responsible for the de-anodization energy. Na_xMnO_2 materials possess the great advantage of the high abundance of sodium resources. Recently, Zuo's team designed an efficient water-mediated system to synthesize P2-$Na_{0.67}MnO_2$ (S-NMO) with a shale structure (Fig. 3),[71] and reported it could regulate the D_{Na^+} effectively. Further, the S-NMO electrodes displayed high cycling (>3000 cycles) and rate capabilities (100 mA h g^{-1}@960 mA g^{-1}); proving that the superior D_{Na^+} has a great influence on the performances of electrodes.

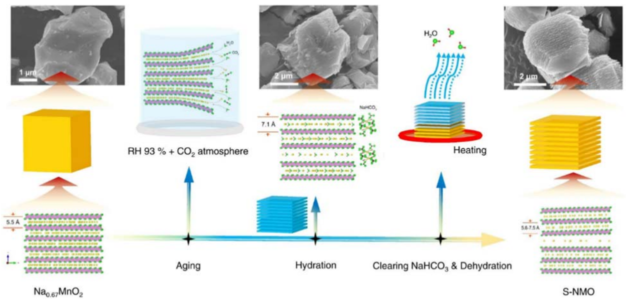

Fig. 3 Synthetic route for preparing S-NMO. Adapted with permission from ref. 71, Copyright {2021} Springer Nature.

2.2 Binary Na_xTMO_2

To address the problems of unitary Na_xTMO_2 (*e.g.*, inferior cycling, poor structural stability, unsatisfactory specific capacity),[72] doping a new TM ion to construct a binary-TM system is an effective strategy. The resulting synergistic effect of the ions can improve the electrochemical/structural stabilities.[73] The Ni^{2+}/Ni^{4+} redox couple can provide a higher working voltage. However, P2-$Na_{0.67}Ni_{0.33}Mn_{0.67}O_2$ usually exhibits disappointing cycle/rate abilities, because of drastic phase transformation and its vulnerable D_{Na^+}.[74] When charged to 4.2 V, $Na_{0.67}Ni_{0.33}Mn_{0.67}O_2$ can undergo P2 → O2 phase transition, which could be observed by the appearance of a new (002′) diffraction peak in the XRD analysis (Fig. 4a).[75] For P2-$Na_{0.67}Ni_{0.33}Mn_{0.67}O_2$, Yang's group systematically studied the optimal synthesis parameters *via* orthogonal experiments,[77] and reported that an excess Na content (3%) is able to effectively improve the capacity (159.3 mA h g^{-1}). Another research study found that the cut-off voltage (up to 4.5 V or low to 1.5 V) could influence the P2–O2 transition and Mn^{4+}/Mn^{3+} redox reaction.[78] Yet another study reported a one-pot method to obtain porous P2-$Na_{0.67}Ni_{0.33}Mn_{0.67}O_2$ microcuboids with the {010} plane exposed,[79] which exhibited good performance (94.6%@1500 cycles@850 mA g^{-1}). Moreover, it was also reported that the design of porous hierarchical P2-$Na_{2/3}Ni_{1/3}Mn_{2/3}O_2$ nanofibers could primarily stabilize the structure as well as stimulate electrochemical reactions,[80] thereby facilitating superb rate abilities (73.4 and 166.7 mA h g^{-1} at 3.4 and 17 mA g^{-1}, respectively) and significantly improved cycling performance (81%@500 cycles). The highly reversible changes in the structure and Ni/Mn redox during cycling were studied by *in situ* XRD and XPS, and it was found that the improved capacity was derived from the $Ni^{2+/3+}$ as well as $Mn^{4+/3+}$ redox reactions (1.5–4.0 V).

Since nickel and cobalt are relatively expensive and toxic, the use of these elements is not conducive to reducing battery costs or for the application of such batteries for large-scale energy

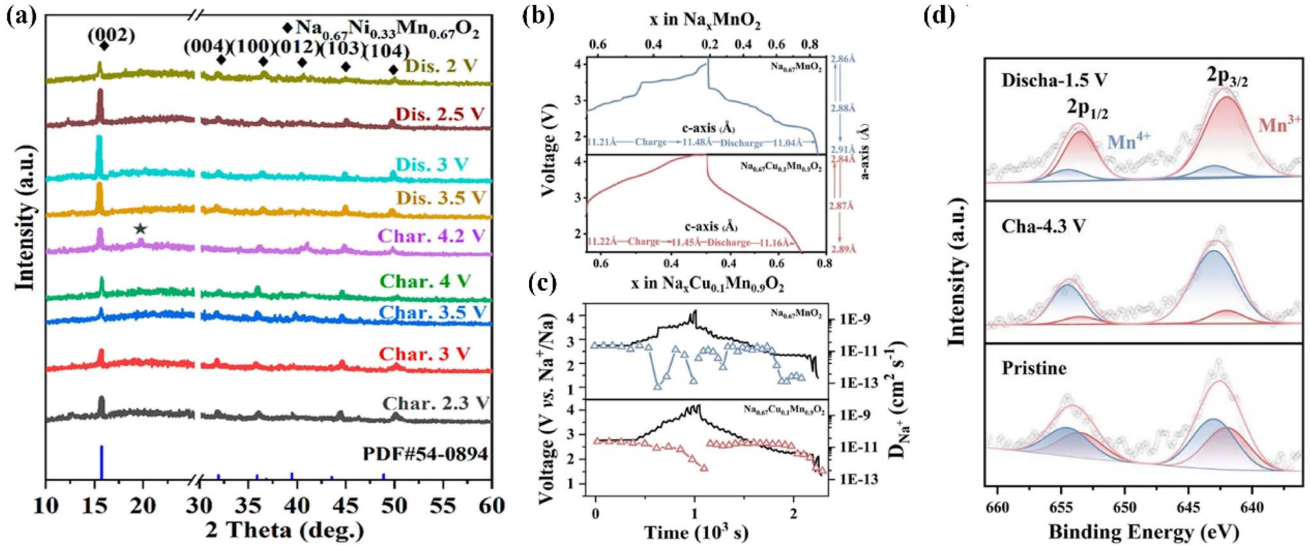

Fig. 4 (a) *Ex situ* XRD of $Na_{0.67}Ni_{0.33}Mn_{0.67}O_2$ in the initial cycle.[75] (b) Calculated lattice parameters from *in situ* XRD; (c) GITT and D_{Na^+} of P2-$Na_{0.67}MnO_2$ and P2-$Na_{0.67}Cu_{0.1}Mn_{0.9}O_2$ electrodes; (d) *ex situ* XPS of P2-$Na_{0.67}Cu_{0.1}Mn_{0.9}O_2$ electrodes in pristine, fully charged and discharged states. Adapted with permission from ref. 76, Copyright {2021} American Chemical Society.

storage. Therefore, Chen's group first investigated the cheap and non-toxic Cu^{2+}/Cu^{3+} redox couple as an alternative with good electrochemical activity.[81] They synthesized P2-$Na_{0.68}Cu_{0.34}Mn_{0.66}O_2$ by a solid-state method, which showed an initial specific capacity of 74.5 mA h g $^{-1}$. Although the specific capacity of this material was slightly low, their work was significant for motivating the exploration of other low-cost and high-specific-capacity cathode materials; for instance, in another study, $Na_{0.67}Cu_{0.1}Mn_{0.9}O_2$ was reported to be able to deliver a high capacity of 222.7 mA h g^{-1}@10 mA g^{-1}@1.5–4.5 V, and 76% capacity retention @1 A g^{-1}@300 cycles.[72] Here, it was reported that the doping of Cu^{2+} could inhibit the consecutive structural transformation and alleviate Jahn–Teller distortion (Fig. 4b–d), thus improving the whole electrochemical performance. This strategy provides a new idea for the development of P2-Na_xTMO_2 materials with structural stability and high energy density.

2.3 Ternary and multi Na_xTMO_2

As a typical P2-type layered structure material, $Na_{0.67}Ni_{0.33}Mn_{0.67}O_2$ (NNMO) has the advantages of a high theoretical specific capacity (173 mA h g^{-1}) and working voltage. However, when charged to 4.2 V, the existence of P2–O3 transition leads to volume changes, resulting in a poor cycle stability.[82] Pahari and coworkers synthesized P2-$Na_{0.67}Ni_{0.17}Ti_{0.16}Mn_{0.67}O_2$ *via* a solid-state reaction method, and reported an initial excellent discharge capacitance (167 mA h g^{-1}@16 mA g^{-1}) at 3.7 V.[83] Also, $Na_{0.67}Fe_{0.3}Mn_{0.3}Co_{0.4}O_2$(NFMC) displayed an excellent cycling performance (retaining 85.5%@100 cycles@160 mA g^{-1}), and high rate capabilities (136.7 and 81.1 mA h g^{-1} at 34 and 850 mA g^{-1}).[84] The NFMC cathode delivered higher voltage plateaus (3.3 V) than that for NFM (2.7 V) as noted through comparing the charge–discharge curves (Fig. 5a). Further, the polarization of the NFMC electrode was greatly decreased (Fig. 5b and c) as the Co substitution increased the D_{Na^+} in the structure.

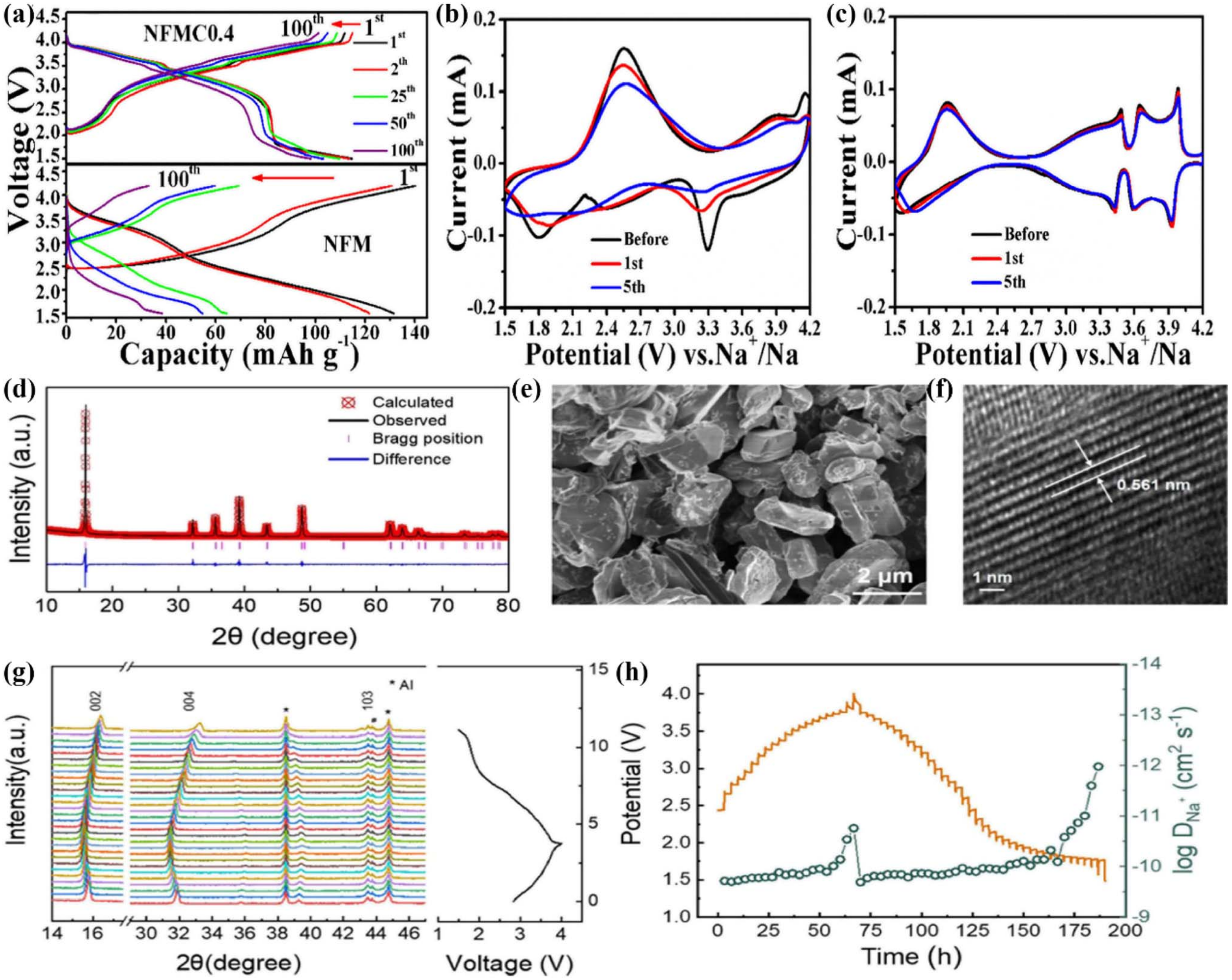

Fig. 5 (a) charge–discharge curves of NFM and NFMC0.4 at 1C. CV curves of (b) NFM and (c) NFMC0.4 at 0.1 mV s^{-1}. Adapted with permission from ref. 84, Copyright {2018} Elsevier B.V. (d) Powder XRD Rietveld refinement pattern; (e) SEM pattern; (f) HRTEM image, and (g) *in situ* XRD at first charge/discharge of P2-NRM at 0.2C. (h) GITT results and the D_{Na^+} coefficient of the NRM material in the first cycle. Adapted with permission from ref. 85, Copyright {2020} American Chemical Society.

In addition, this study revealed that Co substitution could not only effectively enhance the electronic conductivity, but also relieve the polarization of the electrode to some extent.[86]

The electrical performance of NNMO could be effectively promoted to a new and higher level by the co-substitution of two or more transition metals. Compared with NNMO, Cu/Mo co-substituted P2-type $Na_{0.67}Ni_{0.33}Mn_{0.57}Cu_{0.05}Mo_{0.05}O_2$ could effectively inhibit the P2/O2 phase transition, leading to an improvement in the electrochemical performance (142 mA h g^{-1}@2–4.5 V@34 mA g^{-1}@91.5% capacity retention).[87] Peng *et al.* synthesized $[Na_{0.67}Zn_{0.05}]Ni_{0.18}Cu_{0.1}Mn_{0.67}O_2$ by doping Cu^+ at the transition metal site (2a) and the uncommon Zn^+ at the Na site (2d), achieving stable cycling and moisture resistance for the first time.[41] Significantly, *in situ* XRD characterization, and measurements of the charge-transfer kinetics and ion diffusion, as well as microstructural analyses after deep cycling, indicated that the specific two-site doping method could successfully reduce the activation energy of D_{Na^+} in the bulk material, and suppress the formation of O_2 at the end of charging. Doping Zn^+ at the Na site could effectively reduce $d_{(O-Na-O)}$ and enhance the 'pillar' effect of O^{2-}–Zn^{2+}–O^{2-} electrostatic cohesion, thus strengthening the layered cathode structure, and inhibiting the generation of cracks, leading to a superior cycle stability and excellent rate performance. P2-$Na_{0.75}Ni_{1/3}Ru_{1/6}Mn_{1/2}O_2$(NRM) presented a gratifying capacity (161.5 mA h g^{-1}), and excellent cyclic performance (79.5%@500 cycles@10C).[85] The XRD (Fig. 5d) and HRTEM (Fig. 5f) analyses indicated that the material had a layered hexagonal structure of pure P2. As shown in Fig. 5e, NRM particles with diameters in the range of 1–2 μm were uniformly distributed. It could be seen that the (002) and (004) peaks returned to their original positions (Fig. 5g) after the first charging and discharging cycle, indicating the good cycle performance. The maximum diffusion coefficient of Na^+ was 2.05×10^{-10} cm^2 s^{-1} (Fig. 5h), which is higher than that of most P2 materials reported previously,[88] revealing its faster (de)sodiation process and superior rate performance. A comparison of unitary, binary, and multi Na_xTMO_2 is given in Table 2.

3 Problems and optimization of P2-structured materials

3.1 Problems with P2-structured materials

At present, there are still some problems to be solved with P2-cathode materials. For instance, due to the large radius of Na^+, there are obvious kinetic barriers in the migration process and possible effects of structural collapse during the deintercalation/intercalation process, resulting in a poor rate performance and rapid capacity fading in cycling. Besides, the majority of P2-phase materials produce phase transformation when they are charged above 4.2 V, resulting in structural and volume changes.[89] For example, for the P2-$Na_{0.67}Ni_{0.33}Mn_{0.67}O_2$ (P2-NNMO) material, Wang *et al.* found that the main reason for the performance decay was the repeated P2–O2 transitions, which produced an outstanding density of intracrystalline cracks, ultimately destroying the primary grains.[90]

3.2 Lattice doping

Currently, lattice doping can address structural changes by suppressing phase transitions.[91–101] For example, Li^+ doping can improve the Na-storage capacity of cathode materials.[102] For instance, Wang *et al.* engineered large-sized K^+ into the prismatic Na^+ sites of P2-$Na_{0.612}K_{0.056}MnO_2$, resulting in more favorable Na^+ vacancies,[103] which exhibited the highest specific capacity (240.5 mA h g^{-1}@20 mA g^{-1}) and energy density (654 W h kg^{-1}) based on the redox of Mn^{3+}/Mn^{4+}. Cheng's group reported an Al-doped P2-type $Na_{0.6}Ni_{0.3}Mn_{0.7}O_2$ cathode material and investigated the corresponding charge-compensation mechanism.[104] Compared to $Na_{0.6}Ni_{0.3}Mn_{0.7}O_2$, Al doping facilitated the reversible oxygen redox reaction through the reductive coupling reaction between the lone O 2p state in the localized configuration of Na–O–Al and Ni^{4+}. In addition, aluminum doping increased the interlayer spacing and suppressed the disadvantageous P2 → O2 transition during the deiodination/iodination process, which greatly improved the cycling and rate performances. The $Na_{0.67}Ni_{0.31}Mn_{0.67}Y_{0.02}O_2$ material synthesized by Kim *et al.* was found to have strong Y–O bonding, leading to a very stable structure.[105] In addition, it was encased by Y_2O_3, which acted as a protective layer. Due to the large ionic radius of the Y ion (0.90 Å), the atomic charges of Ni, Mn, and O were altered. The Y ion was also used as a protective layer. Meanwhile, Rb^{2+} doping in $Na_{0.78}Ni_{0.32}Mn_{0.68}O_2$ enhanced the mobility of Na^+ and induced atomic-scale surface reorganization, which prevented the transition metals from dissolving into the electrolyte during cycling (Fig. 6a). In particular, it can be seen that it exhibited superior performance with 76% capacity retention at −40 °C (1800 cycles@368 mA g^{-1}) (Fig. 6b). According to the Zn/Mg dual-doping strategy with bifunctional effects, Huang and coworkers synthesized $Na_{0.67}Mn_{0.7}Zn_{0.15}Mg_{0.15}O_2$ *via* a facile co-precipitation method.[97]

Table 2 Comparison of unitary, binary, and multi Na_xTMO_2

Type	Materials	1st capacity (mA h g^{-1})	Lifespan (%@cycles)	Ref.
Unitary	Na_xCoO_2	175	82%@300	70
	$Na_{0.67}MnO_2$	181	79%@3000	71
Binary	$Na_{0.67}Ni_{0.33}Mn_{0.67}O_2$	122	94.6%@1500	79
	$Na_{2/3}Ni_{1/3}Mn_{2/3}O_2$	166.7	81%@500	80
	$Na_{0.67}Cu_{0.1}Mn_{0.9}O_2$	222	76%@300	72
Multi	$Na_{0.67}Fe_{0.3}Mn_{0.3}Co_{0.4}O_2$	136.7	85.5%@100	84
	$Na_{0.67}Ni_{0.33}Mn_{0.57}Cu_{0.05}Mo_{0.05}O_2$	142	91.5%@500	85

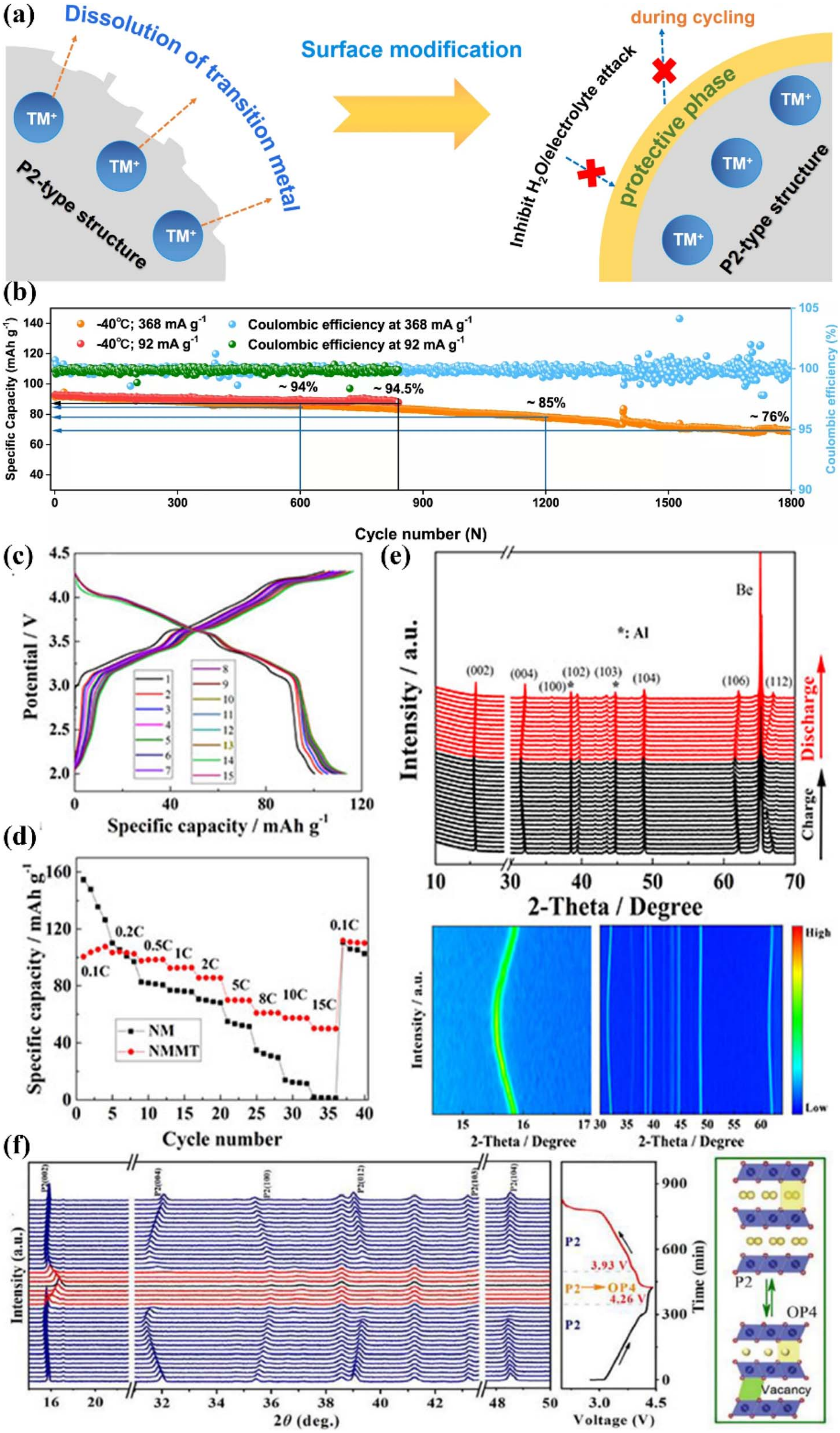

Fig. 6 (a) Schematic showing the protective effect on the main structure *via* surface modification. (b) Long-cycling stability at rates of 92 and 368 mA g^{-1} at −40 °C. Adapted with permission from ref. 106, Copyright {2022} Springer Nature. Charge/discharge profiles of (c) NMMT at 0.1C during the first 15 cycles in the voltage range of 2.0–4.3 V; (d) rate performances of the NMMT cathode; (e) *in situ* XRD tests upon charging/discharging of the NMMT cathode between 2.0 and 4.3 V *versus* Na^+/Na. Adapted with permission from ref. 107, Copyright {2022} American Chemical Society. (f) *In situ* XRD patterns of $NaNMTi_{0.3}OF$ during the first charge/discharge process. Adapted with permission from ref. 108, Copyright {2022} Elsevier B.V.

Compared with P2-$Na_{0.67}MnO_2$ and single-ion (Zn/Mg)-doped specimens, Zn/Mg dual-doping broadens the distance between the crystal planes and supplies a spacious ion-diffusion channel for rapid $D_{Na}{}^+$. It also has less Mn^{3+}/Mn^{4+} and a higher lattice oxygen content, which is instrumental for increasing the structural stability. It was proved that the Zn/Mg dual-doped electrode displayed excellent rate performance (67.2 mA h g^{-1}@1.7 A g^{-1}) and a decent cycling stability (93.8% capacity retention@170 mA g^{-1}@100 cycles). This work thus provides a promising avenue for perfecting the performance enhancement of layered cathode materials. Based on the synergistic effect of Mg and Ti co-doping,[107] Li's group designed and investigated $Na_{2/3}[Ni_{2/9}Mg_{1/9}Mn_{5/9}Ti_{1/9}]O_2$ (NMMT), which displayed an apparent capacity activation during the first cycles (113 mA h g^{-1}@17 mA g^{-1}) (Fig. 6c) and outstanding rate ability (50 mA h g^{-1}@850 m A g^{-1}@500 cycles) between 2.0–4.3 V (Fig. 6d). Furthermore, as shown by the *in situ* XRD characterization (Fig. 6e), single-phase electrochemical reactions occurred during the Na^+ deintercalation.

Based on the Ti^{4+}/F^- co-doping strategy, P2-$Na_{0.67}Ni_{0.33}Mn_{0.37}Ti_{0.3}O_{1.9}F_{0.1}$ showed a much strengthened sodium-storage performance within the 2.0–4.4 V range, including a certain cycling ability (77.2%@300 cycles@300 mA g^{-1}) as well as an excellent rate capability (87.7 mA h g^{-1}@1.02 A g^{-1}).[108] *In situ* XRD (Fig. 6f) analysis showed that the Ti^{4+}/F^- co-doping could inhibit both P2 → O2 transitions and Na^+/vacancy ordering, resulting in fast Na^+ diffusion and a stable phase structure. This study offers a novel idea for the development of layered cathode materials with anion–cation synergetic contributions (Table 3).

3.3 Surface modification

Currently, energy-storage systems with greatly reduced costs and higher stability and safety can be developed *via* doping cations or anions. However, the large structural change in the cycle process can result in rapid capacity deterioration and an inferior cycle life. In addition, the high air sensitivity of systems can have a negative impact on the electrochemical performance. Therefore, researchers have modified the electrode surface to reduce the side reactions between the cathode material and electrolyte during cycling process, so that structural stability, ion diffusion ability and electronic conductivity are improved.[109,110] For instance, a carbon coating can be used to enhance the electrochemical performance, but the inferior mechanical properties of carbon make it harder to improve the cycle stability.[111]

Applying a TMO coating on the surface of a P2 cathode is another active method, which can raise the conductivity and electrochemical performance. It was reported that P2-type $Na_{2/3}Fe_{1/2}Mn_{1/2}O_2$ materials can be synthesized by ultrasonic jet pyrolysis followed by solid-state sintering.[112] In addition, a thin Al_2O_3 layer can be formed on the surface of $Na_{2/3}Fe_{/1/2}Mn_{1/2}O_2$, which inhibits the formation of Na_2CO_3-H_2O and avoids its exposure to air, thus improving the storage performance. Yang *et al.* coated ZnO, a semiconducting material with excellent electrical conductivity, on a P2 layer of $Na_{2/3}Ni_{1/3}Mn_{2/3}O_2$, which could significantly inhibit the peeling phenomenon and maintain the morphology and structure of the electrode well.[113] In addition, part of the Zn^{2+} could finds its way into the transition metal oxide (TMO_2) layer, realizing in an improvement of the crystal stability. Based on the synergistic effect of the ZnO coating and Zn^{2+} doping, the material exhibited excellent cycling performance (75%@200 cycles) and rate performance. To address the defects of the P2-$Na_{0.67}Ni_{0.17}Co_{0.17}Mn_{0.66}O_2$ cathode, a dual modification method incorporating Mg/Ti co-doping and MgO surface coating was reported.[114] The results showed that the P2 structure could be stabilized by Mg^{2+}/Ti^{4+} co-substitution, and that the MgO layer could effectively prevent the surface from being corroded by HF, while promoting Na^+ migration. It displayed a 111.6 mA h g^{-1} initial discharge capacity and retained 90.6% of this at a high current density of 100 mA g^{-1}, which evidently surpassed the performance of $Na_{0.67}Ni_{0.17}Co_{0.17}Mn_{0.66}O_2$. The obvious improvement could be attributed to the synergistic effect of Mg^{2+}/Ti^{4+} co-substitution and the MgO surface coating.

In addition, coating a conductive polymer could also effectively enhance the electrochemical performances. Applying a polydopamine-derived carbon coating was reported to be a significant strategy to improve the interfacial stability of P2-type $Na_{0.80}Ni_{0.22}Zn_{0.06}Mn_{0.66}O_2$.[115] The application of consecutive and homogeneous carbonized PDA (C-PDA) layers with a thickness of ∼5 nm could inhibit Na^+ extraction from the surface of P2-$Na_{0.80}Ni_{0.22}Zn_{0.06}Mn_{0.66}O_2$ particles during the electrode fabrication process and the formation of electrochemically harmful Na_2CO_3/NaOH species. Compared with pristine samples, the material exhibited a higher discharge capacity (124 mA h g^{-1}@12 mA g^{-1}), superior rate capability

Table 3 Typical dopants in P2-type materials

Materials	Dopant	Voltage (V)	1st capacity (mA h g^{-1})	Lifespan (%@cycles)	Ref.
$Na_{0.67}[Li_{0.22}Mn_{0.78}]O_2$	Ni^{2+}	1.5–4.6	160	73%@300	96
$Na_{0.67}MnO_2$	K^+	1.8–4.3	240.5	98.2%@100	103
$Na_{0.67}Ni_{0.33}Mn_{0.67}O_2$	Al^{3+}	1.5–4.5	213.6	58.7%100	104
$Na_{0.67}Ni_{0.33}Mn_{0.67}O_2$	Y^{2+}	2.0–4.5	126.4	63.4%60	105
$Na_{0.78}Ni_{0.32}Mn_{0.68}O_2$	Rb^{2+}	2.4–4.15	96.6	76%@1800	106
$Na_{0.67}MnO_2$	Zn^{2+}/Mg^{2+}	2.0–4.5	166.2	93.8%@100	97
$Na_{2/3}Ni_{1/3}Mn_{2/3}O_2$	Mg^{2+}/Ti^{4+}	2.0–4.3	113	84.3%@500	107
$Na_{0.67}Ni_{0.33}Mn_{0.67}O_2$	Ti^{4+}/F^-	2.0–4.4	140.3	77.2(300)	108

(62 mA h g^{-1}@1536 mA g^{-1}), and excellent cycle stability (90.7% capacity retention@100 cycles). These results show that proper surface protection can prevent the formation of side products, which is crucial to improving the performance of P2 oxide materials. Without sacrificing the high-voltage performance, Yuan *et al.* stabilized the lattice oxygen in a composite material by applying a small amount of Sn substitution and by further protecting the particle surface with a polypyrrole (PPy) coating.[116] The prepared $Na_{0.67}Ni_{0.33}Mn_{0.63}Sn_{0.04}O_2$@PPy (3.3 wt%) composite displayed superb rate performance (137.6/120.0 mA h g^{-1}@10/100 mA g^{-1}) with 82.5% capacity retention (100 mA g^{-1}@100 cycles). The surface particles of the $Na_{0.67}Ni_{0.33}Mn_{0.63}Sn_{0.04}O_2$@PPy (3.3 wt%) composite did not fall off, indicating that the conductive PPy coating could not only improve the cycling stability, but also played a role as a capsule shell, inhibiting particles from falling off and protecting particles from electrolyte erosion. A NASICON-type $NaTi_2(PO_4)_3$ (NTP) nanoshell was coated on the surface of P2-$Na_{0.67}Co_{0.2}Mn_{0.8}O_2$ (NCM) (Fig. 7a) to promote its performance as a new cathode.[117] The NCM@NTP7 sample displayed outstanding electrochemical charge/discharge profiles, with a high capacity (152.4 mA h g^{-1}@34 mA g^{-1}) and 86.7% capacity retention (85 mA g^{-1}@150 cycles) at room temperature. The optimized coating could effectively inhibit side reactions and greatly improve the cyclic stability. Meanwhile, the NTP could accelerate the Na$^+$-migration kinetics of the host material, providing perfect D_{Na^+} channels and a higher electronic conductivity ($R_{ct} = 26.4\ \Omega$, Fig. 7b, $D_G = 4.04 \times 10^{-10}$ cm^2 s^{-1}, Fig. 7c). It is apparent that PPy coating is a viable method for developing stable outstanding voltage transition metal oxide cathode materials. Some typical reported modifications of P2-type materials are listed in Table 4.

3.4 High entropy modification

Recently, the method of building high entropy oxides has been proven to be another possible strategy to improve the performance of O3-layered oxide cathodes.[118–122] The use of high entropy P2-$Na_{0.6}(Ti_{0.2}Mn_{0.2}Co_{0.2}Ni_{0.2}Ru_{0.2})O_2$ can tune the entropic stabilization of the crystal structure and the diffusion activation energy barriers, leading to superior rate performance at a very high rate (68 mA h g^{-1} at 86C).[123] This work demonstrated an advanced fast-charging layered oxide cathode for SIBs. The entropy-tuned P2-$Na_{0.62}Mn_{0.67}Ni_{0.23}Cu_{0.05}Mg_{0.07}Ti_{0.01}O_2$ could expose more {010} active facet and improve the structural stability.[124] The cathode exhibited outstanding electrochemical performance, especially cycling stability (75% capacity retention@2000 cycles@1.2 A g^{-1}). *In situ* HEXRD tests (Fig. 8a) were performed, revealing that no new phase formation or phase transition occurred. Also, the structure evolution was highly reversible during the charging and discharging Na$^+$ (de)intercalation process (Fig. 8b), leading to a superior electrochemical performance. Therefore, high entropy modification represents a new method for advanced P2-layered cathode materials (Table 5).

3.5 Composite phase modification

A composite phase strategy[127–129] (such as P2/P3, P2/O3, and P2/P3/O3) has also been proposed to enhance the electrochemical performance of P2-Na_xTMO_2 (Table 6).

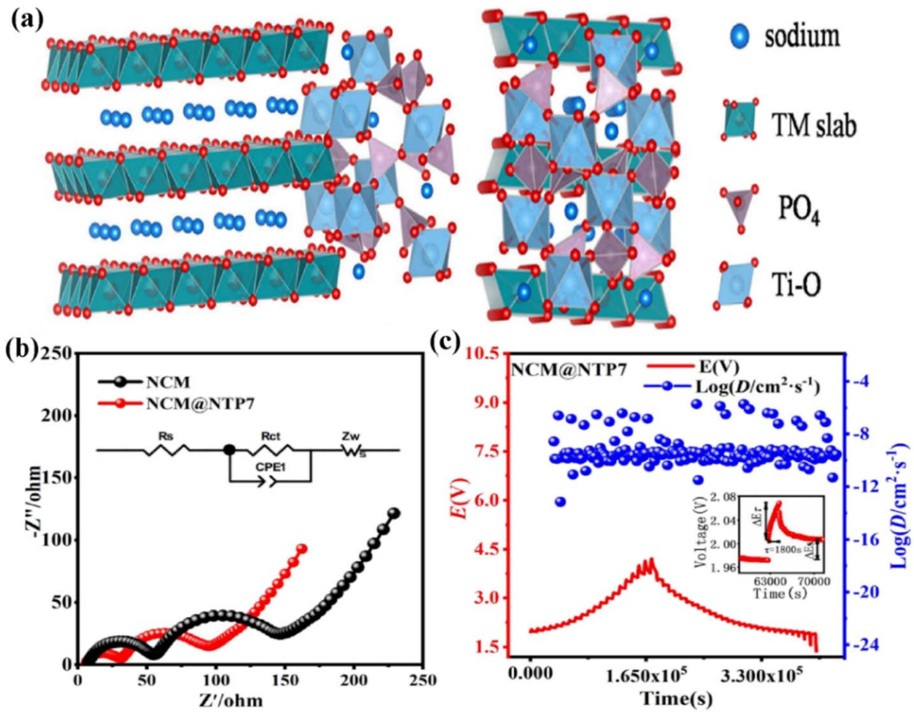

Fig. 7 (a) Interface model of the NCM@NTP7 material; (b) EIS plot, and the inset image shows the equivalent circuit for NCM and NCM@NTP7; GITT curves and corresponding *D* values of (c) NCM@NTP7. Adapted with permission from ref. 117, Copyright {2020} Elsevier B.V.

Table 4 Typical modifications in P2-type materials

Materials	Dopant	Coating	1st capacity (mA h g^{-1})	Lifespan (%@cycles)	Ref.
$Na_{2/3}Fe_{1/2}Mn_{1/2}O_2$		Al_2O_3	146.7	84.7%@40	112
$Na_{2/3}Ni_{1/3}Mn_{2/3}O_2$	Zn^{2+}	ZnO	162	75%@200	113
$Na_{0.67}Ni_{0.17}Co_{0.17}Mn_{0.66}O_2$	Mg^{2+}/Ti^{4+}	MgO	111.6	90.6%@300	114
$Na_{0.80}Ni_{0.28}Mn_{0.66}O_2$	Zn^{2+}	C-PDA	124	62%@100	115
$Na_{0.67}Ni_{0.33}Mn_{0.67}O_2$	Sn^{4+}	PPy	137.6	82.5%@100	116
$Na_{0.67}Co_{0.2}Mn_{0.8}O_2$		$NaTi_2(PO_4)_3$	152.4	86.7%@150	117

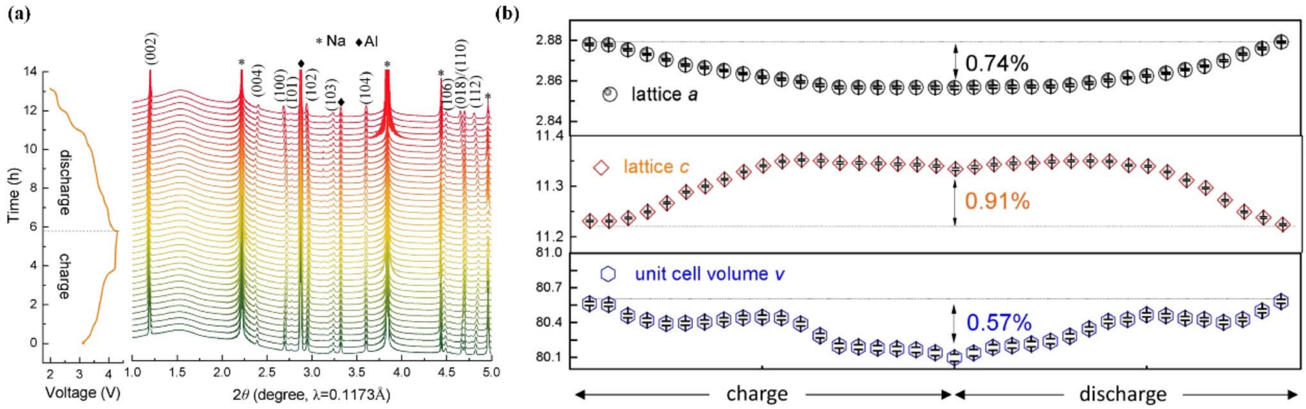

Fig. 8 (a) Waterfall plot of the *in situ* HEXRD patterns for CuMgTi-571 within the range 2.0–4.3 V. (b) Evolution of the cell parameters and cell volume during the charge/discharge process. Adapted with permission from ref. 124, Copyright {2022}, Springer Nature.

Table 5 Typical high-entropy P2-type materials

Materials	Voltage (V)	1st capacity (mA h g^{-1})	Lifespan (%@cycles)	Ref.
$Na_{0.6}(Ti_{0.2}Mn_{0.2}Co_{0.2}Ni_{0.2}Ru_{0.2})O_2$	1.5–4.5	164	70%@40	123
$Na_{0.62}Mn_{0.67}Ni_{0.23}Cu_{0.05}Mg_{0.07}Ti_{0.01}O_2$	2.0–4.3	148	75%@2000	124
$Na_{2/3}[Ni_{1/4}Mn_{1/2}Ti_{1/6}Zn_{1/12}]O_2$	2.5–4.5	114	100%@40	125
$Na_{2/3}Li_{1/6}Fe_{1/6}Co_{1/6}Ni_{1/6}Mn_{1/3}O_2$	2.0–4.5	171	89.3%@90	126

Table 6 Typical multi-phase layered materials for sodium-ion batteries

Materials	Voltage (V)	1st capacity (mA h g^{-1})	Lifespan (%@cycles)	Ref.
P2/P3-$Na_{0.67}Mn_{0.64}Co_{0.30}Al_{0.06}O_2$	1.5–4.0	160	81%@200	130
P2/P3-$Na_{0.5}Mg_{0.2}Co_{0.15}Mn_{0.65}O_2$	1.5–4.3	136	89%@100	131
P2/O3-$Na_{0.76}Ni_{0.33}Mn_{0.50}Fe_{0.10}Ti_{0.07}O_2$	2.2–4.3	144	82%@100	132
P2/O3-$Na_{0.8}Li_{0.2}Ni_{0.33}Mn_{0.67}O_2$	2.0–4.3	133	80%@120	133
P2/O3-$Na_{0.80}Li_{0.13}Ni_{0.20}Fe_{0.10}Mn_{0.57}O_2$	2.0–4.5	172	89%@100	134
P2/O3-$Na_{7/9}Ni_{2/9}Mn_{4/9}Fe_{1/9}Mg_{1/9}Li_{1/9}O_2$	2.0–4.4	170	72.1%@400	135
P3/P2/O3-$Na_{0.674}Ni_{0.319}Mn_{0.590}O_2$	2.0–4.2	100	67%@200	136

Attributed to the fast Na^+ diffusion and stable crystal structure, P2/P3-$Na_{0.67}Mn_{0.64}Co_{0.30}Al_{0.06}O_2$ displayed an outstanding rate capability (83 mA h g^{-1} at 1700 mA g^{-1}) and distinguished cycling stability (81% @200 cycles@1000 mA g^{-1}).[130] *In situ* XRD tests confirmed there were no new peaks except for the P2/P3 phases and that the Jahn–Teller effect was largely relieved during the charge/discharge process, thus realizing a superior long cycling ability. Wang's group explored the sodium-storage mechanism of the P2/O3-$Na_{0.76}Ni_{0.33}Mn_{0.50}Fe_{0.10}Ti_{0.07}O_2$ cathode.[132] *In operando* XRD measurements revealed the reversible structural transformation of P2/O3–P2/O3/P3–P2/P3–P2/Z/O3′–Z/O3′, attributed to the $Ni^{2+}/Ni^{3.5+}$, Fe^{3+}/Fe^{4+}, and

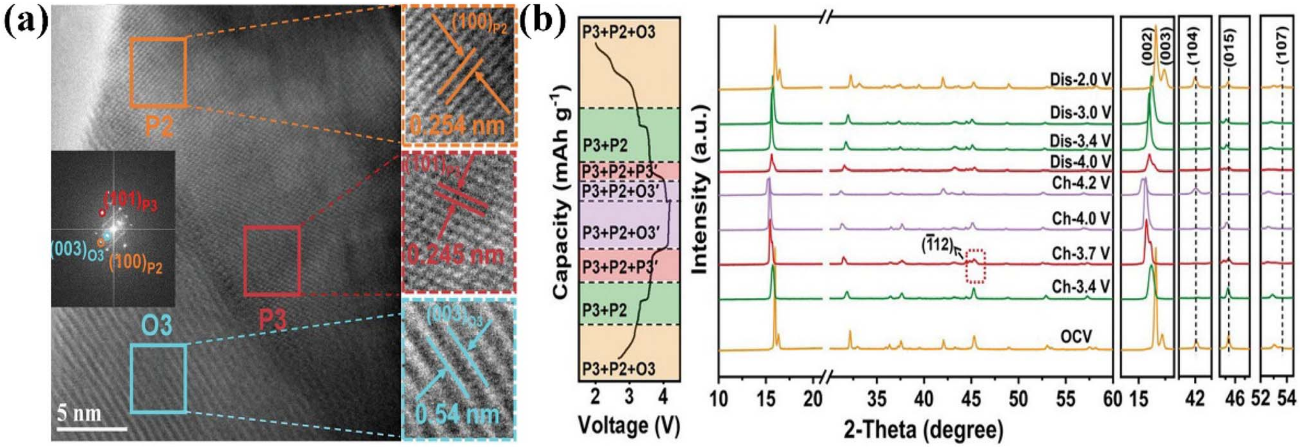

Fig. 9 (a) HRTEM images of P2/P3/O3-NNMO; (b) *ex situ* XRD patterns (right) of P3/P2/O3-NNMO at different voltages between 2.0 and 4.2 V during the first charge/discharge process. Adapted with permission from ref. 136, Copyright {2022}, Wiley-VCH.

$Mn^{3.8+}/Mn^{4+}$ redox couples during the Na^+-(de)intercalation process. This also led to its high capacity (144 mA h g^{-1} at 42 mA g^{-1}) and dramatic rate performance (82 mA h g^{-1} at 210 mA g^{-1}). This work provides a novel idea for the design of high-performance layered multi-phase structures. Because of the staggered arrangement of different phase structures, the P3/P2/O3-$Na_{0.674}Ni_{0.319}Mn_{0.590}O_2$(NNMO) cathode displayed an improved rate performance (100 mA h g^{-1} at 750 mA g^{-1}).[136] The HRTEM image of P3/P2/O3-NNMO clearly showed the co-existence of P2 and O3 phases (Fig. 9a), while *ex situ* XRD (Fig. 9b) revealed that P3/P2/O3-NNMO experienced a reversible conversion process of P3/P2/O3—P3/P2—P3/P2/P3′—P3/P2/O3′—P3/P2/P3′—P3/P2—P3/P2/O3 during the first cycle. Also, the P2–O2 phase transition was inhibited, leading to the improved cycling stability (80 mA h g^{-1}@200 cycles@30 mA g^{-1}). The work offers a model to investigate the independent influence of the structure of the electrode on its electrochemical performance. Therefore, the strategy of composite phase modification provides a new approach to suppress irreversible phase transitions and enhance the performance of layered oxide cathodes.[137]

In summary, the modification methods broadly include structural lattice doping, applying a coating on the surface of the material particles, and composite phase modification. In particular, surface coating can improve the interfacial stability of a material, mitigate the side reactions at the electrode/electrolyte interface, and improve the ionic/electronic conductance at the interface. The drawback is that cladding cannot modulate the lattice, *i.e.*, it cannot regulate the spatial and electronic effects of the internal structure of the material. Conversely, ion doping of the lattice of the electrode material with ions with a different valence and radius can play a role in expanding the ion-diffusion channels, improving the conductivity of the bulk phase of the material, and enhancing the structural stability. Moreover, multi-doping has significant superiority over single doping, such as an enhanced effect from synergistic mechanisms, providing multiple ions with a richer electron cloud density, and the different radii of the different ions, which can endow the structure with stronger toughness.

4 Conclusion and future perspectives

SIBs have developed rapidly in the past decade, but their energy density is still not as good as that of LIBs. Compared to P2-Na_xTMO_2, O3-Na_xTMO_2 has a higher initial sodium content, which can provide more specific capacity in the same voltage range, making it more suitable for full-cell applications. For now, using a composite phase is optimal for a full battery. In addition to this, the dual-modification strategy can promote the electrochemical performance of the material more than a single-modification strategy. For example, the combination of elemental doping and surface capping can not only improve the structural stability, but can also further enhance the conductivity of the material and reduce energy losses during charging and discharging. It is also an effective strategy for full battery performance improvement. Another problem to solve is the problem of high cost of materials. Here, the use of abundant raw materials and simple preparation make P2 layered cathode

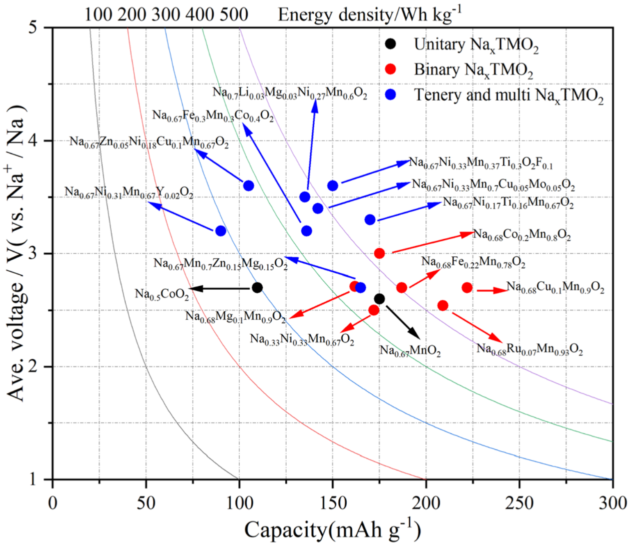

Fig. 10 Gravimetric energy density (W h kg^{-1}) for P2-Na_xMO_2 with different numbers of transition metals in half-cell systems.

materials one of the most competitive cathode materials.[138] Compared with other cathode materials, P2 cathode materials also have the advantages of volume and mass energy density (Fig. 10). From the initial unitary to binary, ternary, and multi metal oxides, the properties of the materials have been further optimized by lattice doping and surface modification, which can also be applied in industry.

Currently, one of the most urgent problems to be solved for this kind of material is to improve the specific capacity of the first charge. The redox reaction of O^{2-} in the structure is an important consideration that could help solve this problem.[139] However, this could incur other problems, such as voltage hysteresis, and poor cycling and rate performance with anionic redox reactions.[140] With the help of some characterization tools (*e.g.*, XANES, XRT, AFM[141] and Cryo-TEM[142]), the redox reaction mechanism of O^{2-} was investigated to provide theoretical guidance for further improving the energy density, cycling, and rate performance of such materials.[143,144]

Although pure-phase P3 type oxides, such as $Na_{2/3}Mg_{1/3}Mn_{2/3}O_2$ and $Na_{2/3}Ni_{1/3}Mn_{2/3}O_2$, have been reported, the P3 phase is more commonly reported as an accompanying impurity for P2 and O3 types. P2-type and P-type $Na_{0.67}MnO_2$ have been shown to exhibit a high reversible capacity and good structural reversibility. However, the initial Na content of P-type layered oxides is relatively low, which is not conducive to assembling the entire battery. Both O3-type and sawtooth-type $NaMnO_2$ have a high initial Na content and specific capacity, but their electrochemical reversibility is poor. The sawtooth-type $NaMnO_2$ is generally accompanied by a mixture of O3-type $NaMnO_2$ phases, and pure sawtooth-type $NaMnO_2$ has not been reported yet.[145,146]

Designing high-entropy layered oxides is another strategy to suppress the P2–O2 phase transition. A transition metal layer composed of various different metal ions can accommodate the local volume changes caused by Na^+ (de)intercalation. Also, the phase transition of high-entropy layered cathodes is highly reversible. Therefore, scientific adjustment of the components and the structure of high entropy layered materials can also contribute to the development of new high-performance cathode materials for sodium-ion batteries. Besides, the low Na content makes it difficult for P2-Na_xTMO_2 to be used in high-energy full-battery systems. So, introducing a certain amount of sodium supplements (such as NaN_3 or Na_3P) can increase the initial sodium content. This could considerably accelerate the industrialization process of SIBs. Otherwise, their poor air stability is another barrier for layered oxide cathodes to attain greater commercialization. To solve this problem, strategies such as nanostructure design, surface coating, and lattice ion doping can be adopted to enhance the air stability and improve the competitiveness of layered cathode materials for large-scale application. Today, there are many other state-of-the-art solutions available for modification. First, sodium-rich layered transition metal oxide cathode materials can be tried out. In these materials, sodium ions occupy the octahedral position of the transition metal layer. In this way, more sodium ions can participate in the reaction and provide more capacity. Second, careful regulation of the ratio of each metal element could be an effective way to improve the structural stability of layered transition metal oxides. Finally, complementary anodes, electrolytes, diaphragms, additives and binders can be developed.

Among these optimization strategies, high-entropy doping designs have been extensively adopted in the last two years, mainly based on a cocktail of effects, entropy-increasing effects, and poly-electron effects, moreover, we believe that a combination of high-entropy doping in different lattice sites with a surface coating strategy may be a practicable solution to simultaneously address issues related to the structural and interface instability, thereby fundamentally making such layered materials have greater practical value for future SIBs.

Data availability

No primary research results, software or code have been included and no new data were generated or analyzed as part of this review.

Author contribution

Manni Li: investigation, formal analysis, writing – original draft. WeiqiLin: investigation, writing – original draft. Yurong Ji: investigation. Lianyu Guan: investigation. Linyuan Qiu: investigation. Yuhong Chen: investigation. Qiaoyu Lu: investigation. Xiang Ding: conceptualization, methodology, writing – review & editing, supervision, funding acquisition.

Conflicts of interest

There are no conflicts to declare.

Acknowledgements

This work was financially supported by the National Natural Science Foundation of China (Grant No. 52102216), the Natural Science Foundation of Fujian Province (Grant No. 2022J01625, 2022-S-002) and the Innovation Training Program for College Students (202310394020, cxxl-2023097, cxxl-2024131, cxxl-2024136).

References

1 X. J. Lin, Y. G. Sun, Y. Liu, K. C. Jiang and A. M. Cao, Stabilization of high-energy cathode materials of metal-ion batteries: Control strategies and synthesis protocols, *Energy Fuels*, 2021, **35**, 7511–7527, DOI: 10.1021/acs.energyfuels.1c00493.

2 T. F. Song and E. Kendrick, Recent progress on strategies to improve the high-voltage stability of layered-oxide cathode materials for sodium-ion batteries, *J. Phys. Mater.*, 2021, **4**, 032004, DOI: 10.1088/2515-7639/abf545.

3 F. L. Wei, Q. P. Zhang, P. Zhang, W. Q. Tian, K. H. Dai, L. Zhang, J. Mao and G. S. Shao, Review-research progress on layered transition metal oxide cathode materials for sodium ion batteries, *J. Electrochem. Soc.*, 2021, **168**, 050524, DOI: 10.1149/1945-7111/abf9bf.

4 V. R. R. Boddu, D. Puthusseri, P. M. Shirage, P. Mathur and V. G. Pol, Layered Na_xCoO_2-based cathodes for advanced Na-ion batteries: Review on challenges and advancements, *Ionics*, 2021, **27**, 4549–4572, DOI: **10.1007/s11581-021-04265-w**.

5 Q. Wang, S. Y. Chu and S. H. Guo, Progress on multiphase layered transition metal oxide cathodes of sodium ion batteries, *Chin. Chem. Lett.*, 2020, **31**, 2167–2176, DOI: **10.1016/j.cclet.2019.12.008**.

6 N. Palaniyandy, Recent developments on layered 3d-transtition metal oxide cathode materials for sodium -ion batteries, *Curr. Opin. Electrochem.*, 2020, **21**, 319–326, DOI: **10.1016/j.coelec.2020.03.023**.

7 Z. Liu, X. Xu, S. Ji, L. Zeng, D. Zhang and J. Liu, Recent Progress of P2-Type Layered Transition-Metal Oxide Cathodes for Sodium-Ion Batteries, *Chem.–Eur. J.*, 2020, **26**, 7747, DOI: **10.1002/chem.201905131**.

8 P. Vanaphuti, Z. Yao, Y. Liu, Y. Lin, J. Wen, Z. Yang, Z. Feng, X. Ma, A. C. Zauha, Y. Wang and Y. Wang, Achieving high stability and performance in P2-type Mn-based layered oxides with tetravalent cations for sodium-ion batteries, *Small*, 2022, **18**, e2201086, DOI: **10.1002/smll.202201086**.

9 Q. N. Liu, Z. Hu, M. Z. Chen, C. Zou, H. L. Jin, S. Wang, S. L. Chou, Y. Liu and S. X. Dou, The cathode choice for commercialization of sodium-ion batteries: Layered transition metal oxides versus prussian blue analogs, *Adv. Funct. Mater.*, 2020, **30**, 1909530, DOI: **10.1002/adfm.201909530**.

10 P. Gupta, S. Pushpakanth, M. A. Haider and S. Basu, Understanding the design of cathode materials for Na-ion batteries, *ACS Omega*, 2022, **7**, 5605–5614, DOI: **10.1021/acsomega.1c05794**.

11 M. Nowak, W. Zając and J. Molenda, Environmentally friendly, inexpensive iron-titanium tunneled oxide anodes for Na-ion batteries, *Energy*, 2022, **239**, 122388, DOI: **10.1016/j.energy.2021.122388**.

12 Y. Zhang, X. Li, X. Chen, R. Koivula and J. Xu, Tunnel manganese oxides prepared using recovered $LiMn_2O_4$ from spent lithium-ion batteries: Co adsorption behavior and mechanism, *J. Hazard. Mater.*, 2022, **425**, 127957, DOI: **10.1016/j.jhazmat.2021.127957**.

13 Z. H. Sun, B. Peng, L. P. Zhao, J. Li, L. Shi and G. Q. Zhang, Constructing layer/tunnel biphasic $Na_{0.6}Fe_{0.04}Mn_{0.96}O_2$ enables simultaneous kinetics enhancement and phase transition suppression for high power/energy density sodium-ion full cell, *Energy Storage Mater.*, 2021, **40**, 320–328, DOI: **10.1016/j.ensm.2021.05.015**.

14 J. Zhang, H. Y. Yuan, Y. P. Huang, S. T. Kan, Y. F. Wu, M. M. Bu, Y. Liu, P. He and H. T. Liu, Engineering sodium-rich manganese oxide with robust tunnel structure for high-performance sodium-ion battery cathode application, *Chem. Eng. J.*, 2021, **417**, 128097, DOI: **10.1016/j.cej.2020.128097**.

15 J. Yin, H. Yang, W. Kong, J. Man, Z. Zhou, W. Feng, J. Sun and Z. Wen, Highly compacted TiO_2/C microspheres via in-situ surface-confined intergrowth with ultra-long life for reversible Na-ion storage, *J. Colloid Interface Sci.*, 2021, **582**, 526–534, DOI: **10.1016/j.jcis.2020.08.060**.

16 Y. Liu and X. Wu, Hydrogen and sodium ions co-intercalated vanadium dioxide electrode materials with enhanced zinc ion storage capacity, *Nano Energy*, 2021, **86**, 106124, DOI: **10.1016/j.nanoen.2021.106124**.

17 C.-J. Yu, Y.-C. Pak, C.-H. Kim, J.-S. Kim, K.-C. Ri, K.-H. Ri, S.-H. Choe and S. Cottenier, Structural and electrochemical trends in mixed manganese oxides $Na_x(M_{0.44}Mn_{0.56})O_2$ (M = Mn, Fe, Co, Ni) for sodium-ion battery cathode, *J. Power Sources*, 2021, **511**, 230395, DOI: **10.1016/j.jpowsour.2021.230395**.

18 L. Rakočević, S. Štrbac, J. Potočnik, M. Popović, D. Jugović and I. S. Simatović, The Na_xMnO_2 materials prepared by a glycine-nitrate method as advanced cathode materials for aqueous sodium-ion rechargeable batteries, *Ceram. Int.*, 2021, **47**, 4595–4603, DOI: **10.1016/j.ceramint.2020.10.025**.

19 B. Peng, J. Gao, Z. Sun, J. Li and G. Zhang, High performance sodium-ion full battery based on one-dimensional nanostructures: The case of $Na_{0.44}MnO_2$ cathode and MoS_2 anode, *J. Phys. D: Appl. Phys.*, 2020, **54**, 014001, DOI: **10.1088/1361-6463/abb8aa**.

20 Q. Liu, Z. Hu, M. Chen, Q. Gu, Y. Dou, Z. Sun, S. Chou and S. X. Dou, Multiangular rod-shaped $Na_{0.44}MnO_2$ as cathode materials with high rate and long life for sodium-ion batteries, *ACS Appl. Mater. Interfaces*, 2017, **9**, 3644–3652, DOI: **10.1021/acsami.6b13830**.

21 M. Qin, W. Ren, R. Jiang, Q. Li, X. Yao, S. Wang, Y. You and L. Mai, Highly crystallized prussian blue with enhanced kinetics for highly efficient sodium storage, *ACS Appl. Mater. Interfaces*, 2021, **13**, 3999–4007, DOI: **10.1021/acsami.0c20067**.

22 J. Peng, W. Zhang, Z. Hu, L. Zhao, C. Wu, G. Peleckis, Q. Gu, J. Z. Wang, H. K. Liu, S. X. Dou and S. Chou, Ice-assisted synthesis of highly crystallized prussian blue analogues for all-climate and long-calendar-life sodium ion batteries, *Nano Lett.*, 2022, **22**, 1302–1310, DOI: **10.1021/acs.nanolett.1c04492**.

23 B. X. Xie, L. G. Wang, H. F. Li, H. Huo, C. Cui, B. Y. Sun, Y. L. Ma, J. J. Wang, G. P. Yin and P. J. Zuo, An interface-reinforced rhombohedral prussian blue analogue in semi-solid state electrolyte for sodium-ion battery, *Energy Storage Mater.*, 2021, **36**, 99–107, DOI: **10.1016/j.ensm.2020.12.008**.

24 J. Peng, W. Zhang, Q. Liu, J. Wang, S. Chou, H. Liu and S. Dou, Prussian blue analogues for sodium-ion batteries: Past, present, and future, *Adv. Mater.*, 2022, **34**, e2108384, DOI: **10.1002/adma.202108384**.

25 Y. Luo, J. Peng and Y. Yan, Self-induced cobalt-derived hollow structure prussian blue as a cathode for sodium-ion batteries, *RSC Adv.*, 2021, **11**, 31827–31833, DOI: **10.1039/d1ra05612c**.

26 S. Kjeldgaard, I. Dugulan, A. Mamakhel, M. Wagemaker, B. B. Iversen and A. Bentien, Strategies for synthesis of prussian blue analogues, *R. Soc. Open Sci.*, 2021, **8**, 201779, DOI: **10.1098/rsos.201779**.

27 W. Jiang, W. T. Qi, Q. Q. Pan, Q. Jia, C. Yang and B. Q. Cao, Potassium ions stabilized hollow Mn-based prussian blue analogue nanocubes as cathode for high performance sodium ions battery, *Int. J. Hydrogen Energy*, 2021, **46**, 4252–4258, DOI: **10.1016/j.ijhydene.2020.10.260**.

28 B. X. Xie, B. Y. Sun, T. Y. Gao, Y. L. Ma, G. P. Yin and P. J. Zuo, Recent progress of prussian blue analogues as cathode materials for nonaqueous sodium-ion batteries, *Coord. Chem. Rev.*, 2022, **460**, 214478, DOI: **10.1016/j.ccr.2022.214478**.

29 Z. Xu, Y. Sun, J. Xie, Y. Nie, X. Xu, J. Tu, C. Shen, Y. Jin, Y. Li, Y. Lu, A. Zhou, F. Chen, T. Zhu and X. Zhao, High-performance Ni/Fe-codoped manganese hexacyanoferrate by scale-up synthesis for practical Na-ion batteries, *Mater. Today Sustain.*, 2022, **18**, 100113, DOI: **10.1016/j.mtsust.2022.100113**.

30 J. Yang, D. Choi, K. S. Kim, D. U. Kim and J. Kim, Poly(vinylalcohol) (pva) assisted sol-gel fabrication of porous carbon network-$Na_3V_2(PO_4)_3$ (NVP) composites cathode for enhanced kinetics in sodium ion batteries, *Polymers*, 2021, **14**, 149, DOI: **10.3390/polym14010149**.

31 S. Wu, L. Wang, Y. Jiang, H. Yang, Y. Wu, Y. Yao, X. Wu and Y. Yu, In situ secondary phase modified low-strain $Na_3Ti(PO_3)_3N$ cathode achieving fast kinetics and ultralong cycle life, *ACS Energy Lett.*, 2022, **7**, 632–639, DOI: **10.1021/acsenergylett.1c02361**.

32 J. X. Wu, C. Lin, Q. H. Liang, G. D. Zhou, J. P. Liu, G. M. Liang, M. Wang, B. H. Li, L. Hu, F. Ciucci, Q. Liu, G. H. Chen and X. L. Yu, Sodium-rich NASICON-structured cathodes for boosting the energy density and lifespan of sodium-free-anode sodium metal batteries, *Infomat*, 2022, **4**, e12288, DOI: **10.1002/inf2.12288**.

33 B. Wu, G. Hou, E. Kovalska, V. Mazanek, P. Marvan, L. Liao, L. Dekanovsky, D. Sedmidubsky, I. Marek, C. Hervoches and Z. Sofer, High-entropy NASICON phosphates $Na_3M_2(PO_4)_3$ and $NaMPO_4O_x$, (M = Ti, V, Mn, Cr, and Zr) for sodium electrochemistry, *Inorg. Chem.*, 2022, **61**, 4092–4101, DOI: **10.1021/acs.inorgchem.1c03861**.

34 R. Guo, W. Li, M. Lu, Y. Lv, H. Ai, D. Sun, Z. Liu and G. C. Han, $Na_3V_2(PO_4)_2F_3$@bagasse carbon as cathode material for lithium/sodium hybrid ion battery, *Phys. Chem. Chem. Phys.*, 2022, **24**, 5638–5645, DOI: **10.1039/d1cp05011g**.

35 P. Salame, K. Kotalgi, M. Devakar and P. More, Electronic transport properties of NASICON structured $NaFe_2(PO_4)(SO_4)(_2)$: A potential cathode material for Na-ion batteries, synthesized using ultrasound-assisted, indirect microwave heating technique, *Mater. Lett.*, 2022, **313**, 131763, DOI: **10.1016/j.matlet.2022.131763**.

36 Y. Y. Zhang, X. Y. Zhu, D. Kai and B. L. Chen, Biomass hyaluronic acid to construct high-loading electrode with fast Na^+ transport structure for $Na_3V_2(PO_4)(_3)$ sodium-ion batteries, *Batteries Supercaps*, 2022, **5**, e202100367, DOI: **10.1002/batt.202100367**.

37 Q. C. Wang, C. Ling, J. B. Li, H. C. Gao, Z. G. Wang and H. B. Jin, Experimental and theoretical investigation of $Na_4MnAl(PO_4)(_3)$ cathode material for sodium-ion batteries, *Chem. Eng. J.*, 2021, **425**, 130680, DOI: **10.1016/j.cej.2021.130680**.

38 L. Y. Shen, Y. Li, S. Roy, X. P. Yin, W. B. Liu, S. S. Shi, X. Wang, X. M. Yin, J. J. Zhang and Y. F. Zhao, A robust carbon coating of $Na_3V_2(PO_4)(_3)$ cathode material for high performance sodium-ion batteries, *Chin. Chem. Lett.*, 2021, **32**, 3570–3574, DOI: **10.1016/j.cclet.2021.03.005**.

39 J. Liu, Y. Huang, Z. Zhao, W. Ren, Z. Li, C. Zou, L. Zhao, Z. Tang, X. Li, M. Wang, Y. Lin and H. Cao, Yeast template-derived multielectron reaction NASICON structure $Na_3MnTi(PO_4)_3$ for high-performance sodium-ion batteries, *ACS Appl. Mater. Interfaces*, 2021, **13**, 58585–58595, DOI: **10.1021/acsami.1c17700**.

40 X. F. Dong, X. L. Zhao, Y. J. Chen and C. Wang, Investigations about the influence of different carbon matrixes on the electrochemical performance of $Na_3V_2(PO_4)(_3)$ cathode material for sodium ion batteries, *Adv. Compos. Hybrid Mater.*, 2021, **4**, 1070–1081, DOI: **10.1007/s42114-021-00319-9**.

41 B. Peng, Y. Chen, F. Wang, Z. Sun, L. Zhao, X. Zhang, W. Wang and G. Zhang, Unusual site-selective doping in layered cathode strengthens electrostatic cohesion of alkali-metal layer for practicable sodium-ion full cell, *Adv. Mater.*, 2022, **34**, e2103210, DOI: **10.1002/adma.202103210**.

42 Z. Zhao, X. Huang, Y. Shao, S. Xu, L. Chen, L. Shi, Q. Yi, C. Shang and D. Zhang, Surface modification of $Na_{0.44}MnO_2$ via a nonaqueous solution-assisted coating for ultra-stable and high-rate sodium-ion batteries, *Chem. Eng. J. Adv.*, 2022, **10**, 100292, DOI: **10.1016/j.ceja.2022.100292**.

43 D. Baster, L. Kondracki, E. Oveisi, S. Trabesinger and H. H. Girault, Prussian blue analogue-sodium-vanadium hexacyanoferrate as a cathode material for Na-ion batteries, *ACS Appl. Energy Mater.*, 2021, **4**, 9758–9765, DOI: **10.1021/acsaem.1c01832**.

44 M. Chen, W. Hua, J. Xiao, J. Zhang, V. W. Lau, M. Park, G. H. Lee, S. Lee, W. Wang, J. Peng, L. Fang, L. Zhou, C. K. Chang, Y. Yamauchi, S. Chou and Y. M. Kang, Activating a multielectron reaction of NASICON-structured cathodes toward high energy density for sodium-ion batteries, *J. Am. Chem. Soc.*, 2021, **143**, 18091–18102, DOI: **10.1021/jacs.1c06727**.

45 C. Delmas, C. Fouassier and P. Hagenmuller, Structural classification and properties of the layered oxides, *Physica. B+C*, 1980, **99**, 81–85, DOI: **10.1016/0378-4363(80)90214-4**.

46 N. Yabuuchi, K. Kubota, M. Dahbi and S. Komaba, Research development on sodium-ion batteries, *Chem. Rev.*, 2014, **114**, 11636–11682, DOI: **10.1021/cr500192f**.

47 X. Rong, E. Hu, Y. Lu, F. Meng, C. Zhao, X. Wang, Q. Zhang, X. Yu, L. Gu, Y.-S. Hu, H. Li, X. Huang, X.-Q. Yang, C. Delmas and L. Chen, Anionic redox reaction-induced high-capacity and low-strain cathode with suppressed phase transition, *Joule*, 2019, **3**, 503–517, DOI: **10.1016/j.joule.2018.10.022**.

48 C. Delmas, Sodium and sodium-ion batteries: 50 years of research, *Adv. Energy Mater.*, 2018, **8**, 1703137, DOI: **10.1002/aenm.201703137**.

49 H. R. Yao, P. F. Wang, Y. Wang, X. Q. Yu, Y. X. Yin and Y. G. Guo, Excellent comprehensive performance of Na-based layered oxide benefiting from the synergetic contributions of multimetal ions, *Adv. Energy Mater.*, 2017, **7**, 1700189, DOI: 10.1002/aenm.201700189.

50 D. D. Yuan, X. H. Hu, J. F. Qian, F. Pei, F. Y. Wu, R. J. Mao, X. P. Ai, H. X. Yang and Y. L. Cao, P2-type $Na_{0.67}Mn_{0.65}Fe_{0.2}Ni_{0.15}O_2$ cathode material with high-capacity for sodium-ion battery, *Electrochim. Acta*, 2014, **116**, 300–305, DOI: 10.1016/j.electacta.2013.10.211.

51 M. Palanisamy, V. R. Reddy Boddu, P. M. Shirage and V. G. Pol, Discharge state of layered P2-type cathode reveals unsafe than charge condition in thermal runaway event for sodium-ion batteries, *ACS Appl. Mater. Interfaces*, 2021, **13**, 31594–31604, DOI: 10.1021/acsami.1c04482.

52 V. R. Reddy Boddu, M. Palanisamy, L. Sinha, S. C. Yadav, V. G. Pol and P. M. Shirage, Hysteresis abated P2-type $NaCoO_2$ cathode reveals highly reversible multiple phase transitions for high-rate sodium-ion batteries, *Sustainable Energy Fuels*, 2021, **5**, 3219–3228, DOI: 10.1039/d1se00490e.

53 A. Ramesh, A. Tripathi and P. Balaya, A mini review on cathode materials for sodium-ion batteries, *Int. J. Appl. Ceram. Technol.*, 2022, **19**, 913–923, DOI: 10.1111/ijac.13920.

54 G. Li and W. Zhu, First-principles investigation on the crystal, electronic structures and diffusion barriers of F-doped $NaMO_2$ (M=V, Cr, Co and Ni) for rechargeable Na-ion batteries, *J. Solid State Chem.*, 2021, **302**, 122440, DOI: 10.1016/j.jssc.2021.122440.

55 F. Geng, Q. Yang, C. Li, B. Hu, C. Zhao, M. Shen and B. Hu, Operando EPR and EPR imaging study on a $NaCrO_2$ cathode: Electronic property and structural degradation with Cr dissolution, *J. Phys. Chem. Lett.*, 2021, **12**, 781–786, DOI: 10.1021/acs.jpclett.0c03327.

56 S. Wang, F. Chen, X. D. He, L. M. Zhang, F. Chen, J. R. Wang, J. M. Dong and C. H. Chen, Self-template synthesis of $NaCrO_2$ submicrospheres for stable sodium storage, *ACS Appl. Mater. Interfaces*, 2021, **13**, 12203–12210, DOI: 10.1021/acsami.0c23069.

57 A. Bhardwaj and A. K. Panwar, Effect of carbon shell over $NaCrO_2$ core by C_2H_2 decomposition to enhance electrochemical properties for rechargeable sodium-ion batteries, *Appl. Surf. Sci.*, 2022, **573**, 151449, DOI: 10.1016/j.apsusc.2021.151449.

58 D. H. Kim, J.-Y. Kim, J.-H. Park, S.-O. Kim, H.-S. Kim, K.-B. Kim and K. Y. Chung, Rt-XAMF and Tr-XRD studies of solid-state synthesis and thermal stability of $NaNiO_2$ as cathode material for sodium-ion batteries, *Ceram. Int.*, 2022, **48**, 19675–19680, DOI: 10.1016/j.ceramint.2022.03.104.

59 S. D. Zhang, M. Y. Qi, S. J. Guo, Y. G. Sun, X. X. Tan, P. Z. Ma, J. Y. Li, R. Z. Yuan, A. M. Cao and L. J. Wan, Advancing to 4.6 V review and prospect in developing high-energy-density $LiCoO_2$ cathode for lithium-ion batteries, *Small Methods*, 2022, **6**, e2200148, DOI: 10.1002/smtd.202200148.

60 Y. C. Lyu, X. Wu, K. Wang, Z. J. Feng, T. Cheng, Y. Liu, M. Wang, R. M. Chen, L. M. Xu, J. J. Zhou, Y. H. Lu and B. K. Guo, An overview on the advances of $LiCoO_2$ cathodes for lithium-ion batteries, *Adv. Energy Mater.*, 2021, **11**, 2000982, DOI: 10.1002/aenm.202000982.

61 J. Zhang, P. F. Wang, P. Bai, H. Wan, S. Liu, S. Hou, X. Pu, J. Xia, W. Zhang, Z. Wang, B. Nan, X. Zhang, J. Xu and C. Wang, Interfacial design for a 4.6 V high-voltage single-crystalline $LiCoO_2$ cathode, *Adv. Mater.*, 2022, **34**, e2108353, DOI: 10.1002/adma.202108353.

62 H. I. Elsaeedy, Synthesis and characterization of $LiCoO_2$ thin films as potential cathode material for lithium-ion batteries, *J. Electron. Mater.*, 2020, **49**, 282–289, DOI: 10.1007/s11664-019-07787-2.

63 N. Yabuuchi, Rational material design of Li-excess metal oxides with disordered rock salt structure, *Curr. Opin. Electrochem.*, 2022, **34**, 100978, DOI: 10.1016/j.coelec.2022.100978.

64 C. Bae, N. Dupre and B. Kang, Further improving coulombic efficiency and discharge capacity in $LiNiO_2$ material by activating sluggish approximately 3.5 V discharge reaction, *ACS Appl. Mater. Interfaces*, 2021, **13**, 23760–23770, DOI: 10.1021/acsami.1c04359.

65 J. Langdon, Z. H. Cui and A. Manthiram, Role of electrolyte in overcoming the challenges of $LiNiO_2$ cathode in lithium batteries, *ACS Energy Lett.*, 2021, **6**, 3809–3816, DOI: 10.1021/acsenergylett.1c01714.

66 J. Xiao, X. Li, K. K. Tang, D. D. Wang, M. Q. Long, H. Gao, W. H. Chen, C. T. Liu, H. Liu and G. X. Wang, Recent progress of emerging cathode materials for sodium ion batteries, *Mater. Chem. Front.*, 2021, **5**, 3735–3764, DOI: 10.1039/d1qm00179e.

67 S. M. Kang, J. H. Park, A. Jin, Y. H. Jung, J. Mun and Y. E. Sung, Na(+)/vacancy disordered P2-$Na_{0.67}Co_{1-x}Ti_xO_2$: High-energy and high-power cathode materials for sodium ion batteries, *ACS Appl. Mater. Interfaces*, 2018, **10**, 3562–3570, DOI: 10.1021/acsami.7b16077.

68 H. Kim, H. Kim, Z. Ding, M. H. Lee, K. Lim, G. Yoon and K. Kang, Recent progress in electrode materials for sodium-ion batteries, *Adv. Energy Mater.*, 2016, **6**, 1600943, DOI: 10.1002/aenm.201600943.

69 L. Gao, S. Chen, H. Hu, H. Y. Cheng, L. L. Zhang and X. L. Yang, Hierarchical Na_xCoO_2 microspheres with low surface area toward high performance sodium ion batteries, *Mater. Lett.*, 2020, **260**, 126965, DOI: 10.1016/j.matlet.2019.126965.

70 Y. Gan, Y. Li, H. Li, W. Qiu and J. Liu, Origin of multiple voltage plateaus in P2-type sodium layered oxides, *Mater. Horiz.*, 2022, **9**, 1460–1467, DOI: 10.1039/D1MH01991K.

71 W. Zuo, X. Liu, J. Qiu, D. Zhang, Z. Xiao, J. Xie, F. Ren, J. Wang, Y. Li, G. F. Ortiz, W. Wen, S. Wu, M. S. Wang, R. Fu and Y. Yang, Engineering Na(+)-layer spacings to stabilize Mn-based layered cathodes for sodium-ion batteries, *Nat. Commun.*, 2021, **12**, 4903, DOI: 10.1038/s41467-021-25074-9.

72 H. R. Shi, J. Y. Li, M. J. Liu, A. P. Luo, L. Y. Li, Z. G. Luo and X. Y. Wang, Multiple strategies toward advanced P2-type layered Na_xMnO_2 for low-cost sodium-ion batteries, *ACS*

Appl. Energy Mater., 2021, **4**, 8183–8192, DOI: **10.1021/acsaem.1c01449**.

73 D. M. Zhou, C. Zeng, J. Xiang, T. Wang, Z. T. Gao, C. L. An and W. X. Huang, Review on Mn-based and Fe-based layered cathode materials for sodium-ion batteries, *Ionics*, 2022, **28**, 2029–2040, DOI: **10.1007/s11581-022-04519-1**.

74 D. Hou, E. Gabriel, K. Graff, T. Li, Y. Ren, Z. Wang, Y. Liu and H. Xiong, Thermal dynamics of P2-$Na_{0.67}Ni_{0.33}Mn_{0.67}O_2$ cathode materials for sodium ion batteries studied by in situ analysis, *J. Mater. Res.*, 2022, **37**, 1156–1163, DOI: **10.1557/s43578-022-00519-z**.

75 J. Feng, S.-h. Luo, J. Wang, P. Li, S. Yan, J. Li, P.-q. Hou, Q. Wang, Y. Zhang and X. Liu, Stable electrochemical properties of magnesium-doped Co-free layered P2-type $Na_{0.67}Ni_{0.33}Mn_{0.67}O_2$ cathode material for sodium ion batteries, *ACS Sustain. Chem. Eng.*, 2022, **10**, 4994–5004, DOI: **10.1021/acssuschemeng.2c00197**.

76 Y. Ling, J. Zhou, S. Guo, H. Fu, Y. Zhou, G. Fang, L. Wang, B. Lu, X. Cao and S. Liang, Copper-stabilized P'2-type layered manganese oxide cathodes for high-performance sodium-ion batteries, *ACS Appl. Mater. Interfaces*, 2021, **13**, 58665–58673, DOI: **10.1021/acsami.1c18313**.

77 L. Yang, Q. Wang, Y. Y. Liu, S. H. Luo, Y. H. Zhang and X. Liu, Optimize solid-state synthesis of P2-$Na_{0.67}Ni_{0.33}Mn_{0.67}O_2$ cathode materials by using the orthogonal experimental design method, *Int. J. Energy Res.*, 2021, **45**, 16865–16873, DOI: **10.1002/er.6843**.

78 Q. Liu, Z. Hu, M. Chen, C. Zou, H. Jin, S. Wang, Q. Gu and S. Chou, P2-type $Na_{2/3}Ni_{1/3}Mn_{2/3}O_2$ as a cathode material with high-rate and long-life for sodium ion storage, *J. Mater. Chem. A*, 2019, **7**, 9215–9221, DOI: **10.1039/C8TA11927A**.

79 B. Peng, Z. H. Sun, L. P. Zhao, S. Y. Zeng and G. Q. Zhang, Shape-induced kinetics enhancement in layered P2-$Na_{0.67}Ni_{0.33}Mn_{0.67}O_2$ porous microcuboids enables high energy/power sodium-ion full battery, *Batteries Supercaps*, 2021, **4**, 388, DOI: **10.1002/batt.202100036**.

80 Y. C. Liu, Q. Y. Shen, X. D. Zhao, J. Zhang, X. B. Liu, T. S. Wang, N. Zhang, L. F. Jiao, J. Chen and L. Z. Fan, Hierarchical engineering of porous P2-$Na_{2/3}Ni_{1/3}Mn_{2/3}O_2$ nanofibers assembled by nanoparticles enables superior sodium-ion storage cathodes, *Adv. Funct. Mater.*, 2020, **30**, 1907837, DOI: **10.1002/adfm.201907837**.

81 S. Y. Xu, X. Y. Wu, Y. M. Li, Y. S. Hu and L. Q. Chen, Novel copper redox-based cathode materials for room-temperature sodium-ion batteries, *Chin. Phys. B*, 2014, **23**, 118202, DOI: **10.1088/1674-1056/23/11/118202**.

82 H. Ren, Y. Li, Q. Ni, Y. Bai, H. Zhao and C. Wu, Unraveling anionic redox for sodium layered oxide cathodes: Breakthroughs and perspectives, *Adv. Mater.*, 2022, **34**, e2106171, DOI: **10.1002/adma.202106171**.

83 D. Pahari and S. Puravankara, On controlling the P2-O2 phase transition by optimal Ti-substitution on Ni-site in P2-type $Na_{0.67}Ni_{0.33}Mn_{0.67}O_2$ (NNMO) cathode for Na-ion batteries, *J. Power Sources*, 2020, **455**, 227957, DOI: **10.1016/j.jpowsour.2020.227957**.

84 D. M. Zhou, W. X. Huang and F. L. Zhao, P2-type $Na_{0.67}Fe_{0.3}Mn_{0.3}Co_{0.4}O_2$ cathodes for high-performance sodium-ion batteries, *Solid State Ionics*, 2018, **322**, 18–23, DOI: **10.1016/j.ssi.2018.04.019**.

85 Q. Wang, K. Jiang, Y. Feng, S. Chu, X. Zhang, P. Wang, S. Guo and H. Zhou, P2-type layered $Na_{0.75}Ni_{1/3}Ru_{1/6}Mn_{1/2}O_2$ cathode material with excellent rate performance for sodium-ion batteries, *ACS Appl. Mater. Interfaces*, 2020, **12**, 39056–39062, DOI: **10.1021/acsami.0c09082**.

86 Y. F. Wen, J. J. Fan, C. G. Shi, P. Dai, Y. H. Hong, R. X. Wang, L. N. Wu, Z. Y. Zhou, J. T. Li, L. Huang and S. G. Sun, Probing into the working mechanism of Mg versus Co in enhancing the electrochemical performance of P2-type layered composite for sodium-ion batteries, *Nano Energy*, 2019, **60**, 162–170, DOI: **10.1016/j.nanoen.2019.02.074**.

87 L. Xue, J. Z. Wang, Y. X. Teng, J. L. Lu and S. Bao, Enhancing the electrochemical performance of P2-type layered cathode by Cu/Mo co-substitution, *Mater. Lett.*, 2021, **303**, 130507, DOI: **10.1016/j.matlet.2021.130507**.

88 K. Jiang, X. Zhang, H. Li, X. Zhang, P. He, S. Guo and H. Zhou, Suppressed the high-voltage phase transition of P2-type oxide cathode for high-performance sodium-ion batteries, *ACS Appl. Mater. Interfaces*, 2019, **11**, 14848–14853, DOI: **10.1021/acsami.9b03326**.

89 J.-P. Parant, R. Olazcuaga, M. Devalette, C. Fouassier and P. Hagenmuller, Sur quelques nouvelles phases de formule Na_xMnO_2 ($x \leq 1$), *J. Solid State Chem.*, 1971, **3**, 1–11, DOI: **10.1016/0022-4596(71)90001-6**.

90 K. Wang, P. F. Yan and M. L. Sui, Phase transition induced cracking plaguing layered cathode for sodium-ion battery, *Nano Energy*, 2018, **54**, 148–155, DOI: **10.1016/j.nanoen.2018.09.073**.

91 J. Zhang, J. B. Kim, J. Zhang, G. H. Lee, M. Chen, V. W. Lau, K. Zhang, S. Lee, C. L. Chen, T. Y. Jeon, Y. W. Kwon and Y. M. Kang, Regulating pseudo-Jahn-Teller effect and superstructure in layered cathode materials for reversible alkali-ion intercalation, *J. Am. Chem. Soc.*, 2022, **144**, 7929–7938, DOI: **10.1021/jacs.2c02875**.

92 X. Li, J. Xu, H. Li, H. Zhu, S. Guo and H. Zhou, Synergetic anion-cation redox ensures a highly stable layered cathode for sodium-ion batteries, *Adv. Sci.*, 2022, e2105280, DOI: **10.1002/advs.202105280**.

93 Y. J. Guo, P. F. Wang, Y. B. Niu, X. D. Zhang, Q. Li, X. Yu, M. Fan, W. P. Chen, Y. Yu, X. Liu, Q. Meng, S. Xin, Y. X. Yin and Y. G. Guo, Boron-doped sodium layered oxide for reversible oxygen redox reaction in Na-ion battery cathodes, *Nat. Commun.*, 2021, **12**, 5267, DOI: **10.1038/s41467-021-25610-7**.

94 X. L. Li, T. Wang, Y. Yuan, X. Y. Yue, Q. C. Wang, J. Y. Wang, J. Zhong, R. Q. Lin, Y. Yao, X. J. Wu, X. Q. Yu, Z. W. Fu, Y. Y. Xia, X. Q. Yang, T. Liu, K. Amine, Z. Shadike, Y. N. Zhou and J. Lu, Whole-voltage-range oxygen redox in P2-layered cathode materials for sodium-ion batteries, *Adv. Mater.*, 2021, **33**, e2008194, DOI: **10.1002/adma.202008194**.

95 Z. W. Cheng, B. Zhao, Y. J. Guo, L. Z. Yu, B. H. Yuan, W. B. Hua, Y. X. Yin, S. L. Xu, B. Xiao, X. G. Han,

P. F. Wang and Y. G. Guo, Mitigating the large-volume phase transition of P2-type cathodes by synergetic effect of multiple ions for improved sodium-ion batteries, *Adv. Energy Mater.*, 2022, **12**, 2103461, DOI: **10.1002/aenm.202103461**.

96 N. Voronina, M. Y. Shin, H. J. Kim, N. Yaqoob, O. Guillon, S. H. Song, H. Kim, H. D. Lim, H. G. Jung, Y. Kim, H. K. Lee, K. S. Lee, K. Yazawa, K. Gotoh, P. Kaghazchi and S. T. Myung, Hysteresis-suppressed reversible oxygen-redox cathodes for sodium-ion batteries, *Adv. Energy Mater.*, 2022, 2103939, DOI: **10.1002/aenm.202103939**.

97 X. Q. Huang, D. L. Li, H. J. Huang, X. Jiang, Z. H. Yang and W. X. Zhang, Fast and highly reversible Na^+ intercalation/extraction in Zn/Mg dual-doped P2-$Na_{0.67}MnO_2$ cathode material for high-performance Na-ion batteries, *Nano Res.*, 2021, **14**, 3531–3537, DOI: **10.1007/s12274-021-3715-2**.

98 X. Wang, X. Yin, X. Feng, Y. Li, X. Dong, Q. Shi, Y. Zhao and J. Zhang, Rational design of $Na_{0.67}Ni_{0.2}Co_{0.2}Mn_{0.6}O_2$ microsphere cathode material for stable and low temperature sodium ion storage, *Chem. Eng. J.*, 2022, **428**, 130990, DOI: **10.1016/j.cej.2021.130990**.

99 J. Jin, Y. Liu, Q. Shen, X. Zhao, J. Zhang, Y. Song, T. Li, X. Xing and J. Chen, Unveiling the complementary manganese and oxygen redox chemistry for stabilizing the sodium-ion storage behaviors of layered oxide cathodes, *Adv. Funct. Mater.*, 2022, 2203424, DOI: **10.1002/adfm.202203424**.

100 M. Zarrabeitia, T. Rojo, S. Passerini and M. Á. Muñoz-Márquez, Influence of the current density on the interfacial reactivity of layered oxide cathodes for sodium-ion batteries, *Energy Technol.*, 2022, **10**, 2200071, DOI: **10.1002/ente.202200071**.

101 A. K. Paidi, W. B. Park, P. Ramakrishnan, S.-H. Lee, J.-W. Lee, K.-S. Lee, H. Ahn, T. Liu, J. Gim, M. Avdeev, M. Pyo, J. I. Sohn, K. Amine, K.-S. Sohn, T. J. Shin, D. Ahn and J. Lu, Unravelling the nature of the intrinsic complex structure of binary-phase Na-layered oxides, *Adv. Mater.*, 2022, 2202137, DOI: **10.1002/adma.202202137**.

102 C. Zhao, Z. Yao, Q. Wang, H. Li, J. Wang, M. Liu, S. Ganapathy, Y. Lu, J. Cabana, B. Li, X. Bai, A. Aspuru-Guzik, M. Wagemaker, L. Chen and Y.-S. Hu, Revealing high Na-content P2-type layered oxides as advanced sodium-ion cathodes, *J. Am. Chem. Soc.*, 2020, **142**, 5742–5750, DOI: **10.1021/jacs.9b13572**.

103 C. Wang, L. Liu, S. Zhao, Y. Liu, Y. Yang, H. Yu, S. Lee, G. H. Lee, Y. M. Kang, R. Liu, F. Li and J. Chen, Tuning local chemistry of P2 layered-oxide cathode for high energy and long cycles of sodium-ion battery, *Nat. Commun.*, 2021, **12**, 2256, DOI: **10.1038/s41467-021-22523-3**.

104 C. Cheng, M. Ding, T. Yan, J. Jiang, J. Mao, X. Feng, T. S. Chan, N. Li and L. Zhang, Anionic redox activities boosted by aluminum doping in layered sodium-ion battery electrode, *Small Methods*, 2022, **6**, e2101524, DOI: **10.1002/smtd.202101524**.

105 S. Kim, K. Min and K. Park, Y-doped P2-type $Na_{0.67}Ni_{0.33}Mn_{0.67}O_2$: A sodium-ion battery cathode with fast charging and enhanced cyclic performance, *J. Alloys Compd.*, 2021, **874**, 160027, DOI: **10.1016/j.jallcom.2021.160027**.

106 Q. Shi, R. Qi, X. Feng, J. Wang, Y. Li, Z. Yao, X. Wang, Q. Li, X. Lu, J. Zhang and Y. Zhao, Niobium-doped layered cathode material for high-power and low-temperature sodium-ion batteries, *Nat. Commun.*, 2022, **13**, 3205, DOI: **10.1038/s41467-022-30942-z**.

107 Z. Y. Li, X. Ma, I. A. Bobrikov, K. Sun, H. Wang, L. He, Y. Li and D. Chen, Unraveling the synergistic effect of mg and Ti codoping to realize an ordered structure and excellent performance for sodium-ion batteries, *ACS Appl. Mater. Interfaces*, 2022, **14**, 7869–7877, DOI: **10.1021/acsami.1c20757**.

108 P. Zhou, J. Zhang, Z. Che, Z. Quan, J. Duan, X. Wu, J. Weng, J. Zhao and J. Zhou, Insights into the enhanced structure stability and electrochemical performance of Ti^{4+}/F^- co-doped P2-$Na_{0.67}Ni_{0.33}Mn_{0.67}O_2$ cathodes for sodium ion batteries at high voltage, *J. Energy Chem.*, 2022, **67**, 655–662, DOI: **10.1016/j.jechem.2021.10.032**.

109 F. Xia, D. Tie, J. Wang, H. L. Song, W. Wen, X. X. Ye, J. S. Wu, Y. L. Hou, X. G. Lu and Y. F. Zhao, Ultrahigh rate and durable sodium-ion storage at a wide potential window via lanthanide doping and perovskite surface decoration on layered manganese oxides, *Energy Storage Mater.*, 2021, **42**, 209–218, DOI: **10.1016/j.ensm.2021.07.020**.

110 X. Feng, Y. Li, Q. Shi, X. Wang, X. Yin, J. Wang, Z. Xia, H. Xiao, A. Chen, X. Yang and Y. Zhao, A comprehensive modification enables the high-rate capability of P2-$Na_{0.75}Mn_{0.67}Ni_{0.33}O_2$ for sodium-ion cathode materials, *J. Energy Chem.*, 2022, **69**, 442–449, DOI: **10.1016/j.jechem.2022.01.032**.

111 N. N. Sinha and N. Munichandraiah, Synthesis and characterization of carbon-coated $LiNi_{1/3}Co_{1/3}Mn_{1/3}O_2$ in a single step by an inverse microemulsion route, *ACS Appl. Mater. Interfaces*, 2009, **1**, 1241–1249, DOI: **10.1021/am900120s**.

112 Y. J. Chang, G. H. Xie, Y. M. Zhou, J. X. Wang, Z. X. Wang, H. J. Guo, B. Z. You and G. C. Yan, Enhancing storage performance of P2-type $Na_{2/3}Fe_{1/2}Mn_{1/2}O_2$ cathode materials by Al_2O_3 coating, *Trans. Nonferrous Met. Soc.*, 2022, 32, 262–272, DOI: **10.1016/S1003-6326(22)65792-3**.

113 Y. Q. Yang, R. B. Dang, K. Wu, Q. Li, N. Li, X. L. Xiao and Z. B. Hu, Semiconductor material ZnO-coated P2-type $Na_{2/3}Ni_{1/3}Mn_{2/3}O_2$ cathode materials for sodium-ion batteries with superior electrochemical performance, *J. Phys. Chem. C*, 2020, **124**, 1780–1787, DOI: **10.1021/acs.jpcc.9b08220**.

114 J. Z. Wang, Y. X. Teng, G. Q. Su, S. Bao and J. L. Lu, A dual-modification strategy for P2-type layered oxide via bulk Mg/Ti co-substitution and MgO surface coating for sodium ion batteries, *J. Colloid Interface Sci.*, 2022, **608**, 3013–3021, DOI: **10.1016/j.jcis.2021.11.028**.

115 J. Y. Xia, W. W. Wu, K. X. Fang and X. H. Wu, Enhancing the interfacial stability of P2-type cathodes by polydopamine-derived carbon coating for achieving performance

improvement, *Carbon*, 2020, **157**, 693–702, DOI: 10.1016/j.carbon.2019.11.011.

116 S. Yuan, J. Qi, M. Jiang, G. Cui, X. Z. Liao, X. Liu, G. Tan, W. Wen, Y. S. He and Z. F. Ma, Improved cycling performance of P2-$Na_{0.67}Ni_{0.33}Mn_{0.67}O_2$ based on Sn substitution combined with polypyrrole coating, *ACS Appl. Mater. Interfaces*, 2021, **13**, 3793–3804, DOI: 10.1021/acsami.0c17080.

117 Y. Li, Q. H. Shi, X. P. Yin, J. Wang, J. Wang, Y. F. Zhao and J. J. Zhang, Construction NASICON-type $NaTi_2(PO_4)_3$ nanoshell on the surface of P2-type $Na_{0.67}Co_{0.2}Mn_{0.8}O_2$ cathode for superior room/low-temperature sodium storage, *Chem. Eng. J.*, 2020, **402**, 126181, DOI: 10.1016/j.cej.2020.126181.

118 K. Walczak, A. Plewa, C. Ghica, W. Zając, A. Trenczek-Zając, M. Zając, J. Toboła and J. Molenda, $NaMn_{0.2}Fe_{0.2}Co_{0.2}Ni_{0.2}Ti_{0.2}O_2$ high-entropy layered oxide–experimental and theoretical evidence of high electrochemical performance in sodium batteries, *Energy Storage Mater.*, 2022, **47**, 500–514, DOI: 10.1016/j.ensm.2022.02.038.

119 J. Chen, Z. Hou, L. Zhang, W. Mao, T. Zhang, X. Zhang and Y. Qian, An advanced medium-entropy substituted tunnel-type $Na_{0.44}MnO_2$ cathode for high-performance sodium-ion batteries, *Inorg. Chem. Front.*, 2023, **10**, 841–849, DOI: 10.1039/D2QI01567F.

120 C. Zhao, F. Ding, Y. Lu, L. Chen and Y.-S. Hu, High-entropy layered oxide cathodes for sodium-ion batteries, *Angew. Chem., Int. Ed.*, 2020, **59**, 264–269, DOI: 10.1002/anie.201912171.

121 C.-C. Lin, H.-Y. Liu, J.-W. Kang, C.-C. Yang, C.-H. Li, H.-Y. T. Chen, S.-C. Huang, C.-S. Ni, Y.-C. Chuang, B.-H. Chen, C.-K. Chang and H.-Y. Chen, In-situ X-ray studies of high-entropy layered oxide cathode for sodium-ion batteries, *Energy Storage Mater.*, 2022, **51**, 159–171, DOI: 10.1016/j.ensm.2022.06.035.

122 H. Deng, L. Liu and Z. Shi, Effect of copper substitution on the electrochemical properties of high entropy layered oxides cathode materials for sodium-ion batteries, *Mater. Lett.*, 2023, **340**, 134113, DOI: 10.1016/j.matlet.2023.134113.

123 L. Yang, C. Chen, S. Xiong, C. Zheng, P. Liu, Y. Ma, W. Xu, Y. Tang, S. P. Ong and H. Chen, Multiprincipal component P2-$Na_{0.6}(Ti_{0.2}Mn_{0.2}Co_{0.2}Ni_{0.2}Ru_{0.2})O_2$ as a high-rate cathode for sodium-ion batteries, *JACS Au*, 2021, **1**, 98–107, DOI: 10.1021/jacsau.0c00002.

124 F. Fu, X. Liu, X. Fu, H. Chen, L. Huang, J. Fan, J. Le, Q. Wang, W. Yang, Y. Ren, K. Amine, S.-G. Sun and G.-L. Xu, Entropy and crystal-facet modulation of P2-type layered cathodes for long-lasting sodium-based batteries, *Nat. Commun.*, 2022, **13**, 2826, DOI: 10.1038/s41467-022-30113-0.

125 K. Kubota, T. Asari and S. Komaba, Impact of Ti and Zn dual-substitution in P2 type $Na_{2/3}Ni_{1/3}Mn_{2/3}O_2$ on Ni-Mn and Na-vacancy ordering and electrochemical properties, *Adv. Mater.*, 2023, 2300714, DOI: 10.1002/adma.202300714.

126 L. Yao, P. Zou, C. Wang, J. Jiang, L. Ma, S. Tan, K. A. Beyer, F. Xu, E. Hu and H. L. Xin, High-entropy and superstructure-stabilized layered oxide cathodes for sodium-ion batteries, *Adv. Energy Mater.*, 2022, **12**, 2201989, DOI: 10.1002/aenm.202201989.

127 Y. Xiao, H.-R. Wang, H.-Y. Hu, Y.-F. Zhu, S. Li, J.-Y. Li, X.-W. Wu and S.-L. Chou, Formulating high-rate and long-cycle heterostructured layered oxide cathodes by local chemistry and orbital hybridization modulation for sodium-ion batteries, *Adv. Mater.*, 2022, **34**, 2202695, DOI: 10.1002/adma.202202695.

128 Z. Liu, C. Zhou, J. Liu, L. Yang, J. Liu and M. Zhu, Phase tuning of P2/O3-type layered oxide cathode for sodium ion batteries via a simple Li/F co-doping route, *Chem. Eng. J.*, 2022, **431**, 134273, DOI: 10.1016/j.cej.2021.134273.

129 B. Xiao, X. Liu, M. Song, X. Yang, F. Omenya, S. Feng, V. Sprenkle, K. Amine, G. Xu, X. Li and D. Reed, A general strategy for batch development of high-performance and cost-effective sodium layered cathodes, *Nano Energy*, 2021, **89**, 106371, DOI: 10.1016/j.nanoen.2021.106371.

130 N. Jiang, Q. Liu, J. Wang, W. Yang, W. Ma, L. Zhang, Z. Peng and Z. Zhang, Tailoring P2/P3 biphases of layered Na_xMnO_2 by co substitution for high-performance sodium-ion battery, *Small*, 2021, **17**, 2007103, DOI: 10.1002/smll.202007103.

131 J.-Y. Li, H.-Y. Hu, L.-F. Zhou, H.-W. Li, Y.-J. Lei, W.-H. Lai, Y.-M. Fan, Y.-F. Zhu, G. Peleckis, S.-Q. Chen, W.-K. Pang, J. Peng, J.-Z. Wang, S.-X. Dou, S.-L. Chou and Y. Xiao, Surface lattice-matched engineering based on in situ spinel interfacial reconstruction for stable heterostructured sodium layered oxide cathodes, *Adv. Funct. Mater.*, 2023, **33**, 2213215, DOI: 10.1002/adfm.202213215.

132 Z. Cheng, X.-Y. Fan, L. Yu, W. Hua, Y.-J. Guo, Y.-H. Feng, F.-D. Ji, M. Liu, Y.-X. Yin, X. Han, Y.-G. Guo and P.-F. Wang, A rational biphasic tailoring strategy enabling high-performance layered cathodes for sodium-ion batteries, *Angew. Chem., Int. Ed.*, 2022, **61**, e202117728, DOI: 10.1002/anie.202117728.

133 J. Feng, S.-h. Luo, J. Cong, K. Li, S. Yan, Q. Wang, Y. Zhang, X. Liu, X. Lei and P.-q. Hou, Synthesis and electrochemical properties of Co-free P2/O3 biphasic $Na_{1-x}Li_xNi_{0.33}Mn_{0.67}O_2$ cathode material for sodium-ion batteries, *J. Electroanal. Chem.*, 2022, **916**, 116378, DOI: 10.1016/j.jelechem.2022.116378.

134 J. Feng, D. Fang, Z. Yang, J. Zhong, C. Zheng, Z. Wei and J. Li, A novel P2/O3 composite cathode toward synergistic electrochemical optimization for sodium ion batteries, *J. Power Sources*, 2023, **553**, 232292, DOI: 10.1016/j.jpowsour.2022.232292.

135 X. Liang and Y.-K. Sun, A novel pentanary metal oxide cathode with P2/O3 biphasic structure for high-performance sodium-ion batteries, *Adv. Funct. Mater.*, 2022, **32**, 2206154, DOI: 10.1002/adfm.202206154.

136 R. Li, J. Gao, J. Li, H. Huang, X. Li, W. Wang, L.-R. Zheng, S.-M. Hao, J. Qiu and W. Zhou, An undoped tri-phase coexistent cathode material for sodium-ion batteries, *Adv.*

Funct. Mater., 2022, **32**, 2205661, DOI: **10.1002/adfm.202205661**.

137 Z. Liu, C. Peng, J. Wu, T. Yang, J. Zeng, F. Li, A. Kucerna, D. Xue, Q. Liu, M. Zhu and J. Liu, Regulating electron distribution of P2-type layered oxide cathodes for practical sodium-ion batteries, *Mater. Today*, 2023, 22–23, DOI: **10.1016/j.mattod.2023.06.021**.

138 Z. Liu, J. Wu, J. Zeng, F. Li, C. Peng, D. Xue, M. Zhu and J. Liu, Co-Free Layered Oxide Cathode Material with Stable Anionic Redox Reaction for Sodium-Ion Batteries, *Adv. Energy Mater.*, 2023, **13**, 2301471, DOI: **10.1002/aenm.202301471**.

139 D. H. Kim and J. M. Lee, Anionic redox reactions in manganese-based binary layered oxides for advanced sodium-ion batteries, *Chem. Mater.*, 2020, **32**, 5541–5549, DOI: **10.1021/acs.chemmater.0c00415**.

140 C. Li, F. Geng and B. Hu, Anionic redox in Na-based layered oxide cathodes: A review with focus on mechanism studies, *Mater. Today Energy*, 2020, **17**, 100474, DOI: **10.1016/j.mtener.2020.100474**.

141 H. Yang, P. Tang, N. Piao, J. Li, X. Shan, K. Tai, J. Tan, H.-M. Cheng and F. Li, In-situ imaging techniques for advanced battery development, *Mater. Today*, 2022, **57**, 279–294, DOI: **10.1016/j.mattod.2022.05.021**.

142 Q. Chang, Y. X. Angel Ng, D. Yang, J. Chen, T. Liang, S. Chen, X. Zhang, Z. Ou, J. Kim, E. H. Ang, H. Xiang and X. Song, Quantifying the morphology evolution of lithium battery materials using operando electron microscopy, *ACS Mater. Lett.*, 2023, 1506–1526, DOI: **10.1021/acsmaterialslett.3c00065**.

143 Z. Liu, J. Shen, S. Feng, Y. Huang, D. Wu, F. Li, Y. Zhu, M. Gu, Q. Liu, J. Liu and M. Zhu, Ultralow Volume Change of P2-Type Layered Oxide Cathode for Na-Ion Batteries with Controlled Phase Transition by Regulating Distribution of Na^+, *Angew. Chem., Int. Ed.*, 2021, **60**, 20960, DOI: **10.1002/anie.202108109**.

144 C. Peng, X. Xu, F. Li, L. Xi, J. Zeng, X. Song, X. Wan, J. Zhao and J. Liu, Recent Progress of Promising Cathode Candidates for Sodium-Ion Batteries: Current Issues, Strategy, Challenge, and Prospects, *Small Struct.*, 2023, **4**, 2300150, DOI: **10.1002/sstr.202300150**.

145 S. Shi, B. Yang, S. Bai, Q. Chen, Z. Liao, W. Wan, J. Liu and S. Zhong, Ti-doped O3-$NaNi_{0.5}Mn_{0.5}O_2$ as high-performance cathode materials for sodium-ion batteries, *Solid State Ionics*, 2024, **411**, 116554, DOI: **10.1016/j.ssi.2024.116554**.

146 Q. Wang, D. Zhou, C. Zhao, *et al.*, Fast-charge high-voltage layered cathodes for sodium-ion batteries, *Nat. Sustain.*, 2024, **7**, 338–347, DOI: **10.1038/s41893-024-01266-1**.